

A Nonlinear and Nonlocal Model for Animal Aggregation

by

Yuelin QI

A thesis submitted to the School of
Graduate and Postdoctoral Studies in
partial fulfillment of the requirements for
the degree of

Master of Science

The Modelling and Computational Science

University of Ontario Institute of Technology (Ontario Tech
University)

Oshawa, Ontario, Canada

September 2022

Copyright © Yuelin QI, 2022

THESIS EXAMINATION INFORMATION

Submitted by Yuelin QI

Master of Science

Thesis title: A Nonlinear and Nonlocal Model for Animal Aggregation

An oral defense of this thesis took place on <Input date here> in front of the following examining committee:

Examining Committee

Chair of Examining Committee	Dr. Greg Lewis
Research Supervisor	Dr. Lennaert van Veen
Research Co-supervisor	Dr. Luciano Buono
Examining Committee Member	Dr. Hendrick de Haan
External Examiner	Dr. Sean Bohun

The above committee determined that the thesis is acceptable in form and content and that a satisfactory knowledge of the field covered by the thesis was demonstrated by the candidate during an oral examination. A signed copy of the Certificate of Approval is available from the School of Graduate and Postdoctoral Studies.

Abstract

An aggregation model is a kind of model used to show the dynamics of the distribution of the population of organisms. Mathematically, we can use a partial differential equation to model the density of an organism at different times and locations. In this paper, we are going to look at a 2+1-dimensional nonlinear and nonlocal aggregation model proposed by Fetecau [8] with an adaptation of a saturation function to the nonlinear term. The nonlinear term represents the interaction between an individual and its neighbours. The saturation function can suppress or amplify the interaction at a low or high level depending on the values of some parameters in the saturation function. We will explore the behaviour of the model with different saturation functions applied.

Keywords: Aggregation Model, Saturation function, Partial Differential Equation

Declaration of Authorship

- I hereby declare that this thesis consists of original work of which I have authored. This is a true copy of the thesis, including any required final revisions, as accepted by my examiners.
- I authorize the University of Ontario Institute of Technology (Ontario Tech University) to lend this thesis to other institutions or individuals for the purpose of scholarly research. I further authorize Ontario Institute of Technology (Ontario Tech University) to reproduce this thesis by photocopying or by other means, in total or in part, at the request of other institutions or individuals for the purpose of scholarly research. I understand that my thesis will be made electronically available to the public.

Signed:

Date:

Statement of Contributions

The work described in Chapter 2 Section 2 was proposed by Professor Lennaert van Veen and Professor Luciano Buono. The whole implementation part of the thesis is completed by myself. I hereby certify that I am the sole author of this thesis and that no part of this thesis has been published or submitted for publication. I have used standard referencing practices to acknowledge ideas, research techniques, or other materials that belong to others.

Dedicated to my family, Prof.
Lennaert van Veen and Prof.
Luciano Buono

Acknowledgements

I would like to acknowledge and give my sincere thanks to my supervisors, Dr. Lennaert van Veen and Dr. Luciano Buono for giving me wonderful learning opportunities and supporting me with invaluable guidance and encouragement. Their patience and wisdom have deeply inspired me on this thesis as well as other school projects.

Besides my supervisors, I would like to thank the rest of my thesis committee, Dr. Greg Lewis, Dr. Hendrick de Haan and Dr. Sean Bohun. Their insightful suggestions and valued questions have helped me significantly to complete this thesis. They were also my graduate courses instructors and what they had taught me is extremely interesting and invaluable to my academic life.

I would like to express my most genuine gratitude to my classmates, Basak and Jaycee, who encourage me with their warm hearts all the time.

I am extremely grateful to my parents for their love, sacrifice and prayers. Also, I would like to thank my good friends Ruth and David, who fulfil my life with laughter.

Contents

Abstract	iii
Declaration of Authorship	iv
Statement of Contributions	v
Acknowledgements	vii
1 Introduction	1
2 Aggregation Model with Saturated Turning Term	4
2.1 Introduction to Fetecau's Model	4
2.2 Adaptation to Saturation in the Interaction Term	9
3 Exponential Time Differencing Scheme	12
3.1 Calculating the Transportation Term	13
3.2 Simulation of the Transportation Term	17
3.3 Applying EDT to the Interaction Term	22
3.4 Calculating the Interaction Term	25
4 Results	28

4.1	Initial condition 1: One Gaussian bump	29
4.2	Initial condition 2: Two Gaussian bumps	36
5	Conclusions	53
	Bibliography	56
	A Histogram of Turning Functions	58
	B Truncation Error of Symmetry during Simulation	66
	C Links of Supplementary Materials	69
C.1	Movies of the Results	69
C.2	Codes for Simulations	70

List of Figures

2.1	The distance kernel indicating the neighbour area which an individual will be attracted or repelled with an individual centered in the middle	5
2.2	the Distance Kernel for Attraction and Repulsion with individual located at the center	7
2.3	The saturation function (2.2.2) when $H = 1.0, \mu = 1.0$ with $\sigma = 0.8, 1, 1.2$	10
3.1	The Initial Condition $u_0(x_1, x_2, \phi) = \exp(\pi(\cos(x_1) + \cos(x_2)))$	17
3.2	The Population Density Plot of $u(x_1, x_2, \phi)$ with only transportation term at $\phi = -\frac{\pi}{2}, 0, \frac{\pi}{4}$ when $t = 0.5, 1$	19
3.3	the Total Population Density $U(X, t)$ with only transportation term when $t = 0, 0.2, 0.4, 0.6, 0.8$ and 1.0 with arrows representing the angles with the highest density at position (x_1, x_2)	21
4.1	the Total Population Density $U(x_1, x_2, t)$ of the model with initial condition (4.1.1) when only transportation term is in effect at $t = 0, 0.5, 1.0, 1.5, 2.0$ and 2.5 . The arrows represent the angles with the highest density at the position (x_1, x_2)	30

4.2	the Total Population Density $U(x_1, x_2, t)$ when no saturation function is applied to the turning function with $q_a = 2, q_r = 0.5$ of the model with initial condition (4.1.1) at $t = 0, 0.5, 1.0, 1.5, 2.0$ and 2.5 . The arrows represent the angles with the highest density at the position (x_1, x_2) .	32
4.3	The Saturation Function (4.1.2) where $H = 5, \mu = 5$ and $\sigma = 1.2$.	33
4.4	the Total Population Density $U(x_1, x_2, t)$ when saturation function (4.1.2) is applied to the turning function with $q_a = 2, q_r = 0.5$ of the model with initial condition (4.1.1) at $t = 0, 0.5, 1.0, 1.5, 2.0$ and 2.5 . The arrows represent the angles with the highest density at the position (x_1, x_2) .	35
4.5	the Total Population Density $U(x_1, x_2, t)$ when no saturation function is applied to the turning function with $q_a = 2, q_r = 0.5$ of the model with initial condition (4.2.1) at $t = 0, 0.5, 1.0, 1.5, 2.0$ and 2.5 . The arrows represent the angles with the highest density at the position (x_1, x_2) .	37
4.6	the Total Population Density $U(x_1, x_2, t)$ when saturation function (4.1.2) is applied to the turning function with $q_a = 2, q_r = 0.5$ of the model with initial condition (4.2.1) at $t = 0, 0.5, 1.0, 1.5, 2.0$ and 2.5 . The arrows represent the angles with the highest density at the position (x_1, x_2) .	39
4.7	The Saturation Function (4.2.2) where $H = 2, \mu = 2$ and $\sigma = 1$	40
4.8	the Total Population Density $U(x_1, x_2, t)$ when saturation function (4.2.2) is applied to the turning function with $q_a = 2, q_r = 0.5$ of the model with initial condition (4.2.1) at $t = 0, 0.5, 1.0, 1.5, 2.0$ and 2.5 . The arrows represent the angles with the highest density at the position (x_1, x_2) .	42

4.9 the Total Population Density $U(x_1, x_2, t)$ when no saturation function is applied to the turning function with $q_a = 4, q_r = 1$ of the model with initial condition (4.2.1) at $t = 0, 0.5, 1.0, 1.5, 2.0$ and 2.5 . The arrows represent the angles with the highest density at the position (x_1, x_2) .	44
4.10 the Total Population Density $U(x_1, x_2, t)$ when saturation function (4.2.2) is applied to the turning function with $q_a = 4, q_r = 1$ of the model with initial condition (4.2.1) at $t = 0, 0.5, 1.0, 1.5, 2.0$ and 2.5 . The arrows represent the angles with the highest density at the position (x_1, x_2) .	46
4.11 The Saturation Function (4.2.3) where $H = 6, \mu = 6$ and $\sigma = 1$	48
4.12 the Total Population Density $U(x_1, x_2, t)$ when saturation function (4.2.3) is applied to the turning function with $q_a = 4, q_r = 1$ of the model with initial condition (4.2.1) at $t = 0, 0.5, 1.0, 1.5, 2.0$ and 2.5 . The arrows represent the angles with the highest density at the position (x_1, x_2) .	49
4.13 The Saturation Function (4.2.4) where $H = 6, \mu = 6$ and $\sigma = 2.5$	50
4.14 the Total Population Density $U(x_1, x_2, t)$ when saturation function (4.2.4) is applied to the turning function with $q_a = 4, q_r = 1$ of the model with initial condition (4.2.1) at $t = 0, 0.5, 1.0, 1.5, 2.0$ and 2.5 . The arrows represent the angles with the highest density at the position (x_1, x_2) .	52
A.1 Turning Function Values for Initial Condition (4.1.1) with saturation function (4.1.2)	59
A.2 Histogram of Turning Function Values for Initial Condition (4.2.1) with saturation function (4.1.2) when $q_a = 2, q_r = 0.5$	60
A.3 Histogram of Turning Function Values for Initial Condition (4.2.1) with saturation function (4.1.2) when $q_a = 2, q_r = 0.5$	61

A.4	Histogram of Turning Function Values for Initial Condition (4.2.1) with saturation function (4.2.2) when $q_a = 2, q_r = 0.5$	62
A.5	Histogram of Turning Function Values for Initial Condition (4.2.1) with saturation function (4.2.2) when $q_a = 4, q_r = 1$	63
A.6	Histogram of Turning Function Values for Initial Condition (4.2.1) with saturation function (4.2.3) when $q_a = 4, q_r = 1$	64
A.7	Histogram of Turning Function Values for Initial Condition (4.2.1) with saturation function (4.2.4) when $q_a = 4, q_r = 1$	65
B.1	The plot of asymmetry vs. dt and N of a model with symmetric initial condition (B.0.1).(A) shows the asymmetry $D(N, dt = 0.05)$ vs. N . (B) shows the asymmetry $D(N = 64, dt)$ vs. dt	67
B.2	The magnitude of relative error at $t = 1$ with symmetric initial condition (B.0.1)	68

Chapter 1

Introduction

In nature, many organisms prefer to live and move in groups. Animal grouping behaviour is also an important topic in both biological and mathematical fields. Many organisms choose to live in groups since it can help them to overcome many difficulties that might be fatal if they live individually [6]. In the sky, there are many bird species tend to form a flock for foraging or migration[9]. In the water, many fishes have a schooling behaviour in which they swim in groups to defend themselves against predators and reduce energy costs for swimming [7, 2]. On the land, many mammals such as kangaroos form groups of different sizes which is beneficial for predator detection and information exchange [4]. It is important to understand and predict any collective behaviour of animals. Since this information can be used to protect these animals and also be able to prepare if the collective behaviour may cause damage to the environment[10].

There are different ways to build an aggregation model to study the collective behaviour of different organisms. One way is to simulate the movement of each individual in the group. In the individual-based models, the movement of each

individual can be determined by formulating the decision rules on how to interact with its neighbours[13].

In this study, we are going to investigate the collective motion of organisms using another modelling method, which the general density of the population at different locations are calculated by setting up a Partial Differential Equation (PDE) instead of simulating the motion of every individual to simulate the behaviour of the groups. In a previous study by Eftimie et al, a PDE which simulates the movement of the organisms in 1-dimension is established in (1.0.1).

$$\begin{aligned}\partial_t u^+(x, t) + \partial_x (\gamma u^+(x, t)) &= -\lambda^+ u^+(x, t) + \lambda^- u^-(x, t) \\ \partial_t u^-(x, t) - \partial_x (\gamma u^-(x, t)) &= \lambda^+ u^-(x, t) - \lambda^- u^-(x, t)\end{aligned}\tag{1.0.1}$$

In the system, u^+ represents the density moving to the right and u^- represents the density moving to the left. The variables x and t stand for the position and time. The parameter γ is the speed of movement. There is a non-linear term λ^\pm which represents the turning rate result from the interaction with neighbours. λ^+ represents the turning rate from right to left and λ^- represents the turning rate from left to right. There are three kinds of interaction forces on an individual generated by its neighbours: attraction, repulsion and alignment. The type of social force generated by a neighbour is determined by the distance from the individual to the neighbour.

In this thesis, we will investigate a two-dimensional aggregation model with two types of interaction forces: attraction and repulsion. The model is based on Fetecau's research [8] with an additional adaptation on the non-linear interaction term. Then we are going to numerically solve the new system using a

combination of the spectral method and exponential time differencing method.

Finally, we will compare the results between the original Fetecau's model and the model with non-linear adaptation to see how the adaptation term influences the system behaviour.

Chapter 2

Aggregation Model with Saturated Turning Term

In this section, the main content is how to make an adaptation of a saturation function to a two-dimensional aggregation model conducted by Fetecau [8]. I will start with a brief description on Fetecau's model, followed by our new adaptation to the non-linear part of the model.

2.1 Introduction to Fetecau's Model

In Fetecau's paper [8], the model is described as:

$$\partial_t u(\phi, X, t) + \gamma e_\phi \cdot \nabla_X u(\phi, X, t) = -\lambda(\phi, X)u(\phi, X, t) + \int_{-\pi}^{\pi} T(\phi, \phi', X) u(\phi', X, t) d\phi' \quad (2.1.1)$$

In this model, there are four terms which represent different actions of the density u at the location $X = (x_1, x_2)$ within the range $[-\frac{L_{space}}{2}, \frac{L_{space}}{2}]$ facing at angle $\phi \in [-\pi, \pi]$ at time t .

We first look at the first term, $\partial_t u(\phi, X, t)$, which represents the change of density u over time t . Then if we look at the second term, $\gamma e_\phi \cdot \nabla_X u(\phi, X, t)$, where $e_\phi = (\cos(\phi), \sin(\phi))$, represents the how the density changes as the individuals at the location X moves in the direction ϕ with speed γ . These two terms form the linear part of the model.

The right-hand side of the model is non-linear which is also called the interaction terms. These two terms are the result of the density change from the interaction with neighbours. The third term $-\lambda(X, \phi)u(\phi, X, t)$ represents the density move out of the position X at angle ϕ , where $\lambda(X, \phi)$ is the reorientation function. The last term $\int_{-\pi}^{\pi} T(\phi, \phi', X) u(\phi', X, t) d\phi'$ is the density which moves into X at ϕ . The function $T(\phi, \phi', X)$ is a turning function which represents the turning rate of changing from direction ϕ' to ϕ at X .

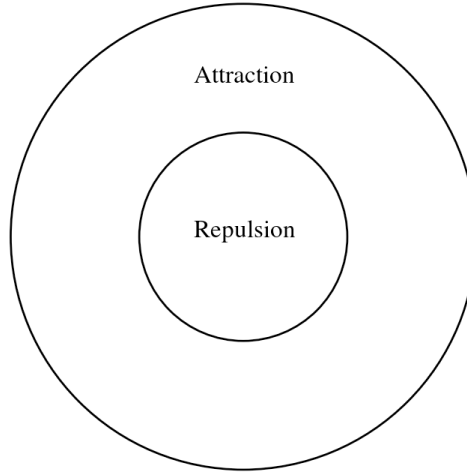


FIGURE 2.1: The distance kernel indicating the neighbour area which an individual will be attracted or repelled with an individual centered in the middle

The turning function is represented as:

$$T(\phi, \phi', X) = T_a(\phi, \phi', X) + T_r(\phi, \phi', X) \quad (2.1.2)$$

$$T_j(\phi, \phi', X) = q_j \int_{\mathbb{R}^2} \int_{-\pi}^{\pi} K_j^d(X - S) K_j^o(\phi', X - S) w_j(\phi, \phi', X - S) u(S, \theta, t) d\theta dS \quad (2.1.3)$$

where q_j is a constant stands for the strength of the turning function.

To explain the turning function $T_j(\phi, \phi', X)$ and the reorientation function $\lambda(X, \phi)$, we first define the distance kernel K_j^d and the orientation kernel K_j^o for both attractive or repulsive interactions ($j = a, r$). The distance kernel K_j^d represents how far the sights of individuals can reach, which is represented in Figure 2.1. Usually, individuals do not like their neighbours to be too close to them, thus the repulsion distance kernel is the area directly surrounding the individual. The attraction distance kernel is the direct opposite, where an individual does not want to stay too far away from their neighbour, thus the attraction distance kernel is placed at some distance from the center. Let X be the individual's position and S be the neighbour's position and $X - S = (s_1, s_2)$, then the distance kernel can be written as:

$$K_j^d(X - S) = \frac{1}{A_j} e^{-\left(\sqrt{s_1^2 + s_2^2} - d_j\right)^2 / m_j^2} \quad (2.1.4)$$

where $j = a, r$ represents whether the distance kernel is for attraction or repulsion, and $A_j = \pi m_j \left(m_j e^{-d_j^2 / m_j^2} + \sqrt{\pi} d_j + \sqrt{\pi} d_j \operatorname{erf}(d_j / m_j) \right)$ is a constant makes $\int_{\mathbb{R}^2} K_j^d d(X - S) = 1$. In (2.1.4), d_j is the interaction range and the m_j is the width of the interaction range. In Figure 2.2 it shows the K_a^d and K_r^d with

the same m_j but different d_j .

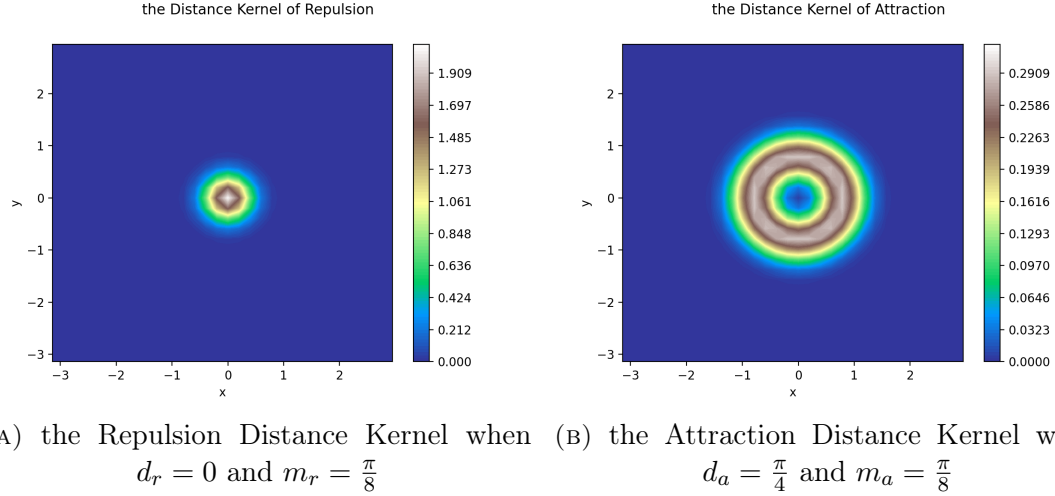


FIGURE 2.2: the Distance Kernel for Attraction and Repulsion with individual located at the center

The other kernel is the orientation kernel, K_j^o , which depends on the individual's angle ϕ' and the angle between the individual's and neighbour's position ψ . The angle ψ can be calculated as

$$\cos \psi = \frac{s_1}{\sqrt{s_1^2 + s_2^2}}, \quad \sin \psi = \frac{s_2}{\sqrt{s_1^2 + s_2^2}} \quad (2.1.5)$$

Then the orientation kernel for attraction and repulsion is:

$$K_a^o(\phi' - \psi) = \frac{1}{2\pi}(-\cos(\phi' - \psi) + 1) \quad (2.1.6)$$

$$K_r^o(\phi' - \psi) = \frac{1}{2\pi}(\cos(\phi' - \psi) + 1) \quad (2.1.7)$$

where for attraction, the orientation kernel maximizes when ψ is at the opposite of ϕ' ($\phi' - \psi = \pi$); for repulsion, the orientation kernel maximizes when ψ is close

to the angle ϕ' ($\phi' - \psi = 0$). Then the total kernel for attraction and repulsion is:

$$K_j(\phi', X - S) = K_j^d(X - S)K_j^o(\phi', X - S) \quad (2.1.8)$$

Another component of the Turning function is the probability function $w_j(\phi, \phi', X - S)$. This gives the probability of the individuals moving from ϕ' to ϕ with the interaction between their neighbours.

$$w_j(\phi, \phi', X - S) = g_\sigma \left(\phi' - \phi - \kappa_j (\sin(\phi' - \psi)) \right) \quad (2.1.9)$$

where

$$g_\sigma(\theta) = \frac{1}{\sqrt{\pi}\sigma} \sum_{z \in \mathbb{Z}} e^{-\left(\frac{\theta+2\pi z}{\sigma}\right)^2}, \quad \theta \in (-\pi, \pi) \quad (2.1.10)$$

is an approximation of periodic Gaussian function with $0 < \kappa_a \leq 1$ and $-1 \leq \kappa_r < 0$. The value of $|\kappa_j|$ represents the influence of the neighbours and σ represents the width of the probability function. We can combine the Kernel and probability function to form a new function

$$Kw_j(\phi, \phi', X - S) = K_j(\phi', X - S)w_j(\phi, \phi', X - S) \quad (2.1.11)$$

Thus, the turning function is a convolution over the spacial parameter $X = (x_1, x_2)$. Let $\int_{-\pi}^{\pi} u(S, \theta, t)d\theta = U(S, t)$, the turning function can be rewritten as:

$$T_j(\phi, \phi', X) = q_j \int_{\mathbb{R}^2} Kw_j(\phi, \phi', X - S) U(S, t) dS \quad (2.1.12)$$

with q_j represents the strength of the specific attractive or repulsive turning functions. The total turning function is

$$T(\phi, \phi', X) = T_a(\phi, \phi', X) + T_r(\phi, \phi', X) \quad (2.1.13)$$

For the reorientation term $\lambda(\phi, X)$, it can also be written in terms of the turning function, where

$$\lambda(\phi, X) = \lambda_a(\phi, X) + \lambda_r(\phi, X) \quad (2.1.14)$$

$$\lambda_j(\phi, X) = \int_{-\pi}^{\pi} T_j(\phi, \phi', X) d\phi \quad (2.1.15)$$

which represents the total volume changing away from the original angle ϕ' .

2.2 Adaptation to Saturation in the Interaction Term

In addition to the original model, there is a new adaptation, a new Saturation function $S(x)$ added to the Turning function. Therefore, the non-linear interaction term $N(\phi, X)$ becomes

$$\begin{aligned} N(\phi, X) &= -\lambda'(\phi, X)u(\phi, X, t) + \int_{-\pi}^{\pi} S(T(\phi, \phi', X)) u(\phi', X, t) d\phi' \\ &= -\int_{-\pi}^{\pi} S(T_j(\phi, \phi', X)) d\phi u(\phi, X, t) + \int_{-\pi}^{\pi} S(T(\phi, \phi', X)) u(\phi', X, t) d\phi' \end{aligned} \quad (2.2.1)$$

In this paper, the saturation function is calculated in the form of

$$S(T) = \frac{H}{2} \left(1 + \tanh \left(\frac{T - \mu}{\sigma} \right) \right) \quad (2.2.2)$$

There are three parameters in the saturation function, which are H , μ and σ . H represents the maximum value of the function, μ relates the midpoint of the function, and σ stands for the width of the function. By applying the saturation function, it simulates the scenario where sometimes an individual does not prefer to interact with its neighbours and limits the influence of the interaction term or there is a stimulus during the interaction.

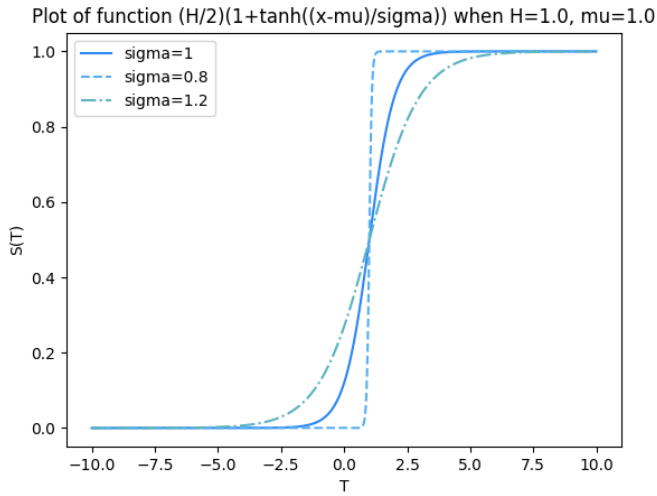


FIGURE 2.3: The saturation function (2.2.2) when $H = 1.0, \mu = 1.0$
with $\sigma = 0.8, 1, 1.2$

In Figure 2.3, it shows a plot of a saturation function. From the plot, we can tell that there are three main sections in a saturation function: maximum section, slope section and minimum section. On the right side of the picture, we can see that the value reaches its maximum at the value $H = 1.0$ with a very small slope.

Similarly, on the left side of the plot, the function also approaches its minimum value 0 with a decreasing slope approaching 0. In the middle part of the section, we can see that with different values of σ , the slope is also different. With a smaller width σ , the slope section becomes steeper and with a greater width σ , the slope becomes smaller.

To make the mass conserved over time, we also need to change the $\lambda(\phi, X)$ since the saturation function is applied to the turning function $T(\phi, \phi', X)$. Now if we integrate over the space and angle to the model with saturation term, the change of the total mass $U(t)$ can be written as

$$\begin{aligned} \frac{dU}{dt} = & - \int_{\mathbb{R}^2} \int_{\phi'=-\pi}^{\pi} \lambda'(\phi', X) u(\phi', X, t) d\phi' dX \\ & + \int_{\mathbb{R}^2} \int_{\phi=-\pi}^{\pi} \int_{\phi'=-\pi}^{\pi} S(T(\phi, \phi', X)) u(\phi', X, t) d\phi' d\phi dX \end{aligned} \quad (2.2.3)$$

To make the mass conserved, where $\frac{dU}{dt} = 0$, then the λ' would become:

$$\lambda'(\phi', X) = \int_{\phi=-\pi}^{\pi} S(T(\phi, \phi', X)) d\phi \quad (2.2.4)$$

Therefore, the new Model with the saturation term is

$$\partial_t u(\phi, X, t) + \gamma e_\phi \cdot \nabla_X u(\phi, X, t) = -\lambda'(X, \phi) u(\phi, X, t) + \int_{-\pi}^{\pi} S(T(\phi, \phi', X)) u(\phi', X, t) d\phi' \quad (2.2.5)$$

Chapter 3

Exponential Time Differencing Scheme

In this chapter, the main time stepping method is introduced and applied to solve the equation over time. In this study, a method named Exponential Time Differencing Scheme and developed by Matthews and Cox is applied [3]. Exponential Time Differencing Scheme is applied to solve an ODE involving both linear and non-linear terms, which can be generalized as:

$$\frac{du(t)}{dt} = Lu(t) + N(u(t), t) \quad (3.0.1)$$

where L is a linear operator acting on $u(t)$ and $N(u(t), t)$ is the non-linear term.

To solve the ODE in (3.0.1), we first state an integrating factor $\mu = \exp(-Lt)$ and multiply both sides of (3.0.1) by μ to get a new equation

$$\frac{d}{dt}(\exp(-Lt)u(t)) = \exp(-Lt)N(u(t), t) \quad (3.0.2)$$

Suppose at the current time step t' , the non-linear term $N(u(t'), t')$ is known as a constant and if we integrate both sides over $(t', t' + \Delta t)$, the equation (3.0.2) becomes:

$$\exp(-Lt)u(t)\Big|_{t'}^{t'+\Delta t} = N(u(t'), t') \int_{t'}^{t'+\Delta t} \exp(-Lt)dt \quad (3.0.3)$$

Finally, the density at the new time step $u(t' + \Delta t)$ can be calculated as

$$u(t' + \Delta t) = \exp(L\Delta t)u(t') + (\exp(L\Delta t) - 1)N(u(t'), t') \quad (3.0.4)$$

3.1 Calculating the Transportation Term

This section will mainly be focusing on simulating the transportation term using Exponential Time Differencing (ETD) scheme. For the interaction terms all equal to zero, the equation can be simplified as

$$u_t + \gamma \mathbf{e}_\phi \cdot \nabla_x u = 0 \quad (3.1.1)$$

To simulate the gradient of u over the space, we can apply the semidiscrete Fourier transform. To simplify the function into a non-dimensional setting, we choose the range of the space $[-\frac{L_{space}}{2}, \frac{L_{space}}{2}]$ with $L_{space} = 2\pi$. Then we can apply the Fourier transform:

$$\hat{u}_{k_1, k_2}(\phi, t) = \alpha \int_{x_2=-\pi}^{\pi} \int_{x_1=-\pi}^{\pi} u(\phi, x_1, x_2, t) \exp(-i[k_1 x_1 + k_2 x_2]) dx_1 dx_2 \quad (3.1.2)$$

where k_1, k_2 are the wave number corresponding to x_1, x_2 . The inverse Fourier transform is

$$u(x_1, x_2, \phi, t) = \beta \sum_{k_1=-\frac{N}{2}}^{\frac{N}{2}} \sum_{k_2=-\frac{N}{2}}^{\frac{N}{2}} \hat{u}_{k_1, k_2}(\phi, t) \exp(i[k_1 x_1 + k_2 x_2]) \quad (3.1.3)$$

where N is the discrete grid number and α, β are the normalization term during the transformation. To solve the function numerically, we are going to apply the spectral method where we can apply Fast Fourier Transform and Inverse Fast Fourier Transform over a space grid with grid number N [12]. Then we can get a coefficient matrix which does not change over time. The calculation of the coefficient matrix will be explained in the following paragraphs.

If Fourier transform over the space is applied to (3.1.1), then $\nabla_x \hat{u} = (ik_1 \hat{u}, ik_2 \hat{u})$. Therefore, the equation becomes

$$\frac{\partial \hat{u}_{k_1, k_2}(\phi, t)}{\partial t} + i\gamma [k_1 \cos(\phi) + k_2 \sin(\phi)] \hat{u}_{k_1, k_2}(\phi, t) = 0 \quad (3.1.4)$$

Suppose that k_1, k_2 be known constants, and discretize ϕ over a grid between $[-\pi, \pi]$ with an even number m points such that $\phi_j = \frac{2\pi}{m}j$ with $j = -\frac{m}{2}, \dots, \frac{m}{2} - 1$, the linear operator at the angle ϕ_j would be $L = -i\gamma[k_1 \cos(\phi_j) + k_2 \sin(\phi_j)]$. If we define $\hat{u}_{k_1, k_2, j} \equiv \hat{u}_{k_1, k_2}(\phi_j, t)$, (3.1.4) can be written as an ODE

$$\frac{d\hat{u}_{k_1, k_2, j_1}(t)}{dt} = \sum_{j_2=-\frac{m}{2}}^{\frac{m}{2}-1} M_{p_1, p_2} \hat{u}_{k_1, k_2, j_2} \quad (3.1.5)$$

where $j_1, j_2 \in (-\frac{m}{2}, \frac{m}{2})$ and $p_1 = j_1 + \frac{m}{2}$, $p_2 = j_2 + \frac{m}{2}$. Then M is a diagonal matrix having entries $M_{p_1, p_2} = L(k_1, k_2, \phi_{j_1})\delta_{j_1, j_2}$ with δ_{j_1, j_2} be the Dirac delta

function. Then if we omit the known constants k_1, k_2 , the system would become

$$\frac{d}{dt} \begin{bmatrix} \hat{u}_{-\frac{m}{2}} \\ \hat{u}_{-\frac{m}{2}+1} \\ \vdots \\ \hat{u}_{\frac{m}{2}-1} \end{bmatrix} = \begin{bmatrix} L(\phi_{-\frac{m}{2}}) & 0 & \cdots & 0 \\ 0 & L(\phi_{-\frac{m}{2}+1}) & \ddots & \vdots \\ \vdots & \ddots & \ddots & 0 \\ 0 & \cdots & 0 & L(\phi_{\frac{m}{2}-1}) \end{bmatrix} \begin{bmatrix} \hat{u}_{-\frac{m}{2}} \\ \hat{u}_{-\frac{m}{2}+1} \\ \vdots \\ \hat{u}_{\frac{m}{2}-1} \end{bmatrix} \quad (3.1.6)$$

where

$$M = \begin{bmatrix} L(\phi_{-\frac{m}{2}}) & 0 & \cdots & 0 \\ 0 & L(\phi_{-\frac{m}{2}+1}) & \ddots & \vdots \\ \vdots & \ddots & \ddots & 0 \\ 0 & \cdots & 0 & L(\phi_{\frac{m}{2}-1}) \end{bmatrix} \quad (3.1.7)$$

To solve the system (3.1.6), we can apply the ETD scheme, where we set the integrating factor $\mu = \exp(-Mt)$, and the system can be simplified as

$$\frac{d}{dt}(\exp(-Mt)\hat{u}) = 0 \quad (3.1.8)$$

If we integrate both sides over the current time step t' and the new time step $t' + \Delta t$ to get

$$\exp(-M(t' + \Delta t))\hat{u}(t' + \Delta t) - \exp(-M(t'))\hat{u}(t') = 0 \quad (3.1.9)$$

the right-hand side remains zero since the non-linear term equals zero. Then to solve for $u(t' + \Delta t)$ the equation becomes

$$\hat{u}(t' + \Delta t) = \exp(M\Delta t)\hat{u}(t') \quad (3.1.10)$$

Finally, the inverse Fourier transform (stated in (3.1.3)) is applied to (3.1.10) to find the density function $u(t' + \Delta t)$ in real space.

3.2 Simulation of the Transportation Term

In this section, we are going to apply the EDT scheme to an initial condition of u

$$u_0(x_1, x_2, \phi) = \exp(\pi(\cos(x_1) + \cos(x_2))) \quad (3.2.1)$$

which is shown in Figure 3.1.

The Initial Condition $u_0(x_1, x_2, \phi) = \exp(\cos(x_1) + \cos(x_2))$

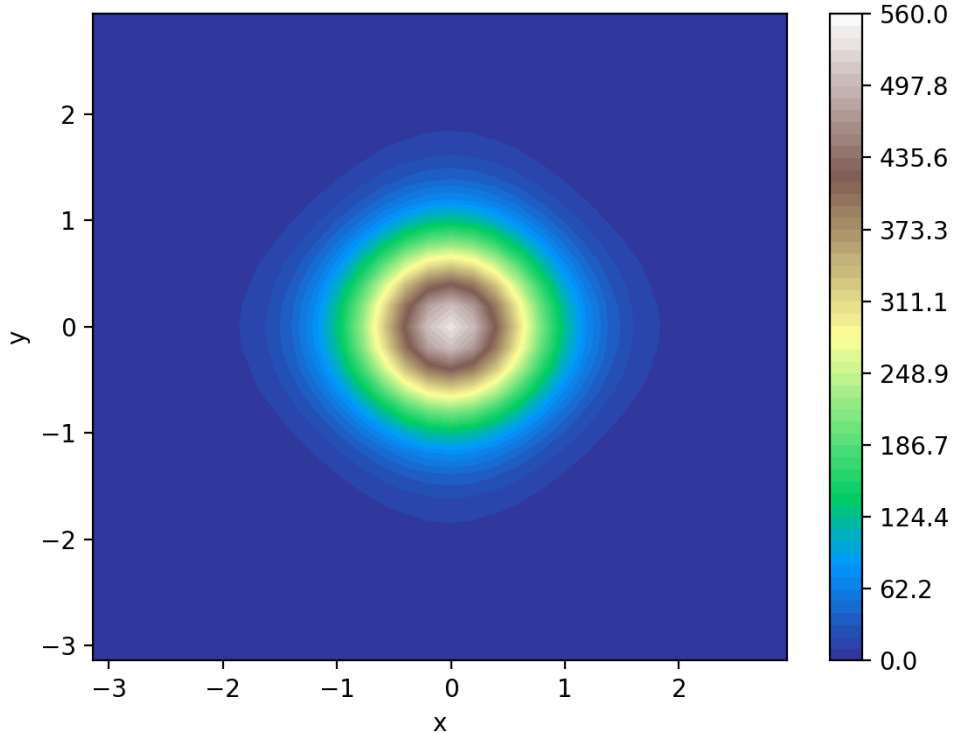
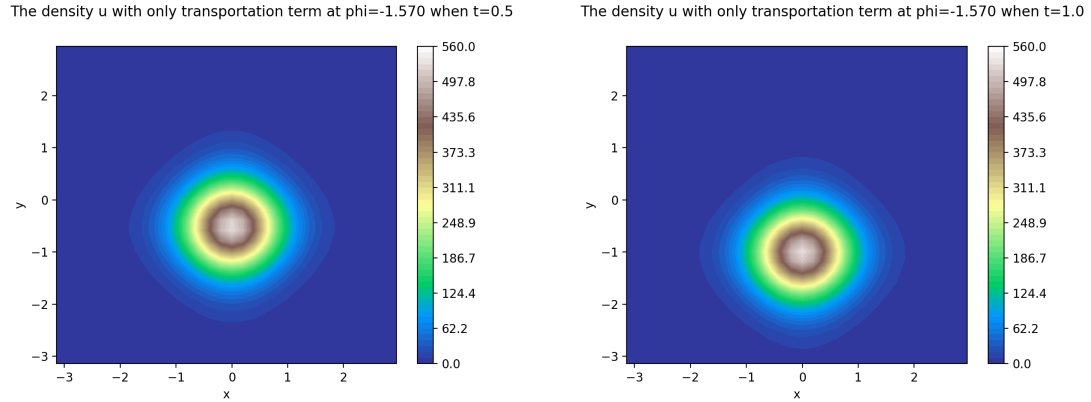
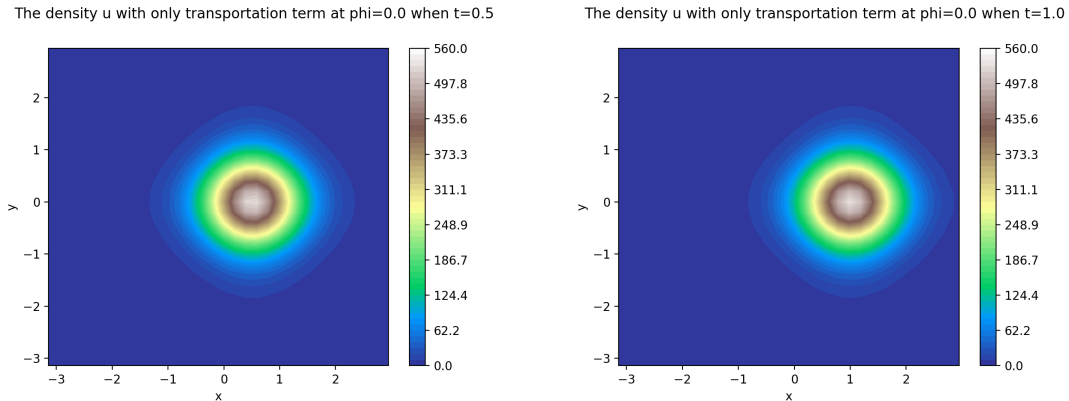
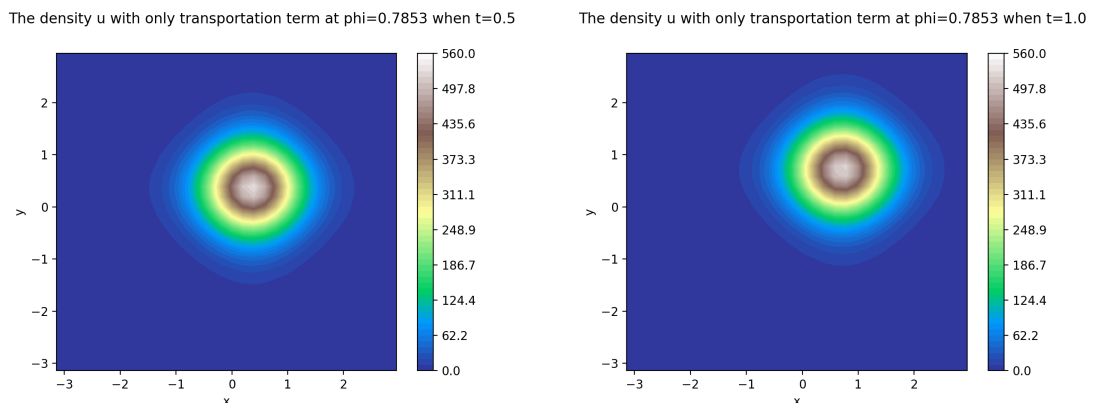


FIGURE 3.1: The Initial Condition $u_0(x_1, x_2, \phi) = \exp(\pi(\cos(x_1) + \cos(x_2)))$

The initial condition u_0 stays the same for different ϕ . But as the time variable t gets larger, since the population is moving toward different directions, the density

plot is also different at different ϕ (Figure 3.2).

(A) The Population Density Plot of $u(x_1, x_2, \phi = -\frac{\pi}{2})$ at $t = 0.5, 1$ (B) The Population Density Plot of $u(x_1, x_2, \phi = 0)$ at $t = 0.5, 1$ (C) The Population Density Plot of $u(x_1, x_2, \phi = \frac{\pi}{4})$ at $t = 0.5, 1$ FIGURE 3.2: The Population Density Plot of $u(x_1, x_2, \phi)$ with only transportation term at $\phi = -\frac{\pi}{2}, 0, \frac{\pi}{4}$ when $t = 0.5, 1$

We can also look at the whole population density plot over different angles, where we define the whole population $U(x_1, x_2, t)$ as

$$U(x_1, x_2, t) = \int_{-\pi}^{\pi} u(x_1, x_2, \phi, t) d\phi \quad (3.2.2)$$

Also, let the arrows at the position x_1, x_2 represent the angle ϕ_{max} with the largest population. The thickness of the arrows varies with different density, where the thicker arrows represent a greater magnitude of density at $u(x_1, x_2, \phi_{max}, t)$. The plot is shown in Figure 3.3. In Figure 3.3, the initial population is concentrated in the center. Then the population starts to spread out from the center toward different directions.

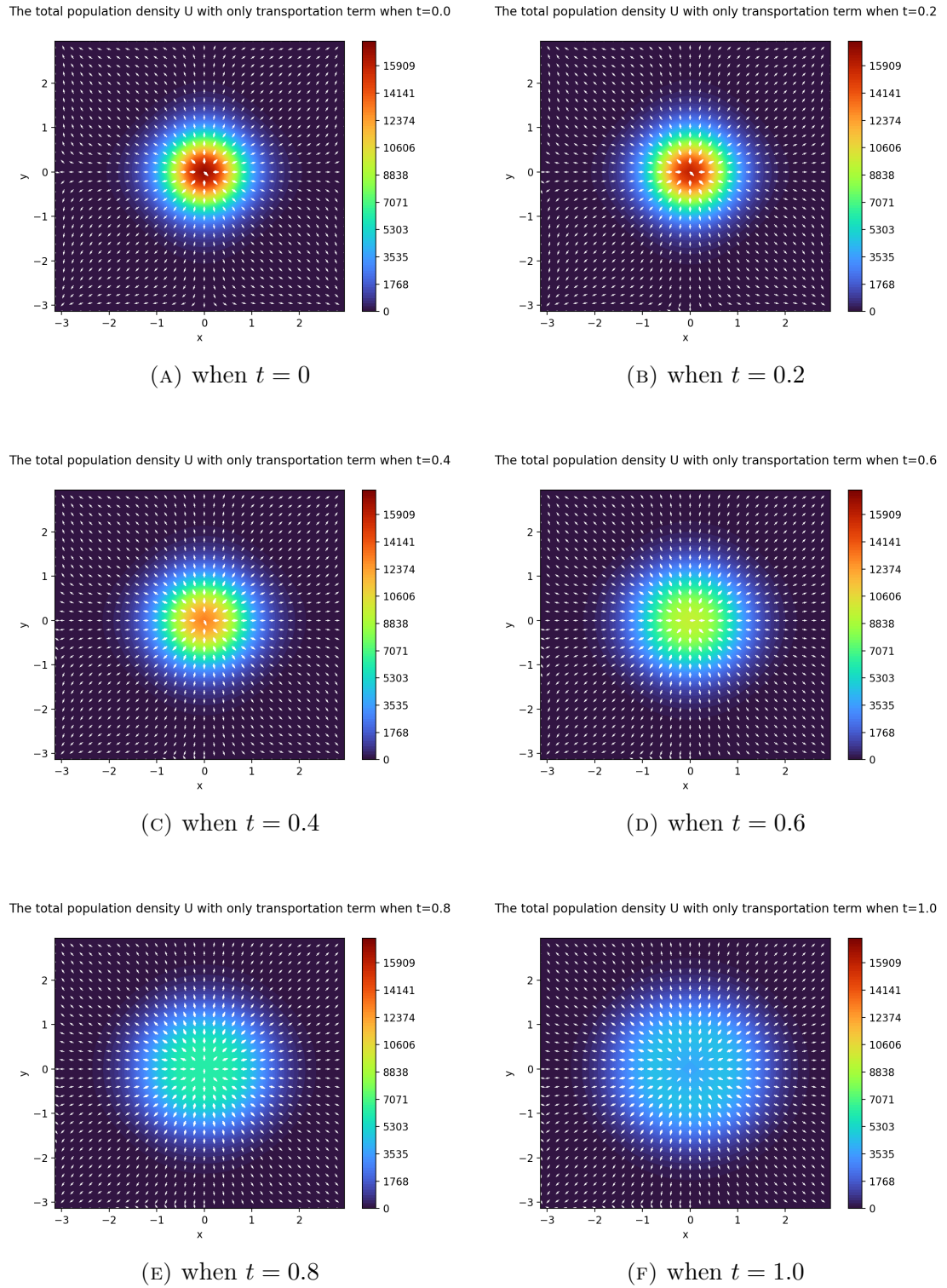


FIGURE 3.3: the Total Population Density $U(X, t)$ with only transportation term when $t = 0, 0.2, 0.4, 0.6, 0.8$ and 1.0 with arrows representing the angles with the highest density at position (x_1, x_2)

3.3 Applying EDT to the Interaction Term

This section will show how to apply the ETD scheme to the interaction term, which is the non-linear part in the equation.

$$N(u(t), t) = -\lambda'(\phi, x_1, x_2)u(\phi, x_1, x_2, t) + \int_{\phi'=-\pi}^{\pi} S(T(\phi, \phi', x_1, x_2)) u(\phi', x_1, x_2, t) d\phi' \quad (3.3.1)$$

Similar to the transportation term, to apply the ETD method, we need to transform the interaction term into Fourier space over the space variable (x_1, x_2) , which can be written as

$$\hat{N}_{k_1, k_2}(t) = \alpha \int_{x_2=-\pi}^{\pi} \int_{x_1=-\pi}^{\pi} N(\phi, x_1, x_2, t) \exp(-i[k_1 x_1 + k_2 x_2]) dx_1 dx_2 \quad (3.3.2)$$

Then the equation in the Fourier space becomes

$$\frac{\partial \hat{u}_{k_1, k_2}(\phi, t)}{\partial t} + i\gamma [k_1 \cos(\phi) + k_2 \sin(\phi)] \hat{u}_{k_1, k_2}(\phi, t) = \hat{N}_{k_1, k_2}(t) \quad (3.3.3)$$

which can be approximated by set an intergrating factor $\mu = \exp(-Mt)$ where the matrix M is the same matrix in (3.1.5). Then the system becomes

$$\frac{d}{dt}(\exp(-Mt)\hat{u}) = \exp(-Mt)\hat{N}_{k_1, k_2}(t) \quad (3.3.4)$$

Then if we integrate both sides over the current time step t' and the new time step $t' + \Delta t$, the equation becomes

$$\exp(-M[t + \Delta t])\hat{u}(t + \Delta t) - \exp(-Mt)\hat{u}(t) = \int_{t'=t}^{t+\Delta t} \exp(-Mt') \hat{N}_{k_1, k_2}(t') dt' \quad (3.3.5)$$

To approximate the non-linear term, one thing is to make the assumption that the function $\hat{N}_{k_1, k_2}(t) = \hat{N}_{k_1, k_2} + \mathcal{O}(\Delta t)$, which is a constant value of the interaction term at a specific time t . Then the integration part can be calculated as

$$\begin{aligned} \int_{t'=t}^{t+\Delta t} \exp(-Mt') \hat{N}_{k_1, k_2}(t') dt' &= \int_{t'=t}^{t+\Delta t} \exp(-Mt') \hat{N}_{k_1, k_2} dt' + \mathcal{O}(\Delta t) \\ &= -M^{-1} (\exp(-M(t + \Delta t)) - \exp(-M(t))) \hat{N}_{k_1, k_2} + \mathcal{O}(\Delta t) \end{aligned}$$

If the result is substitute into (3.3.5), then

$$\hat{u}(t + \Delta t) = \exp(M\Delta t)\hat{u} + M^{-1}(\exp(M\Delta t) - \mathbb{I})\hat{N}_{k_1, k_2} + \mathcal{O}(\Delta t) \quad (3.3.6)$$

To simplify the expression, we can define two diagonal matrices A and B so that the diagonal entries are

$$A_{j,j} = \exp\left(-i\gamma\Delta t [k_1 \cos(\phi_j) + k_2 \sin(\phi_j)]\right) \quad (3.3.7)$$

$$B_{j,j} = \frac{\exp(-i\gamma\Delta t [k_1 \cos(\phi_j) + k_2 \sin(\phi_j)]) - 1}{-i\gamma [k_1 \cos(\phi_j) + k_2 \sin(\phi_j)]} \quad (3.3.8)$$

To avoid dividing by 0 when $k_1, k_2 = 0$ in matrix B , we multiply the entry by 1 in the form of

$$\begin{aligned} c_{j,j} &= \exp\left(\frac{-\Delta t}{2} M_{j,j}\right)^{-1} \exp\left(\frac{-\Delta t}{2} M_{j,j}\right) \\ &= \frac{\exp\left(\frac{i}{2}\gamma\Delta t[k_1\cos(\phi_j) + k_2\sin(\phi_j)]\right)}{\exp\left(\frac{i}{2}\gamma\Delta t[k_1\cos(\phi_j) + k_2\sin(\phi_j)]\right)} \end{aligned} \quad (3.3.9)$$

If we let $Q_{j,j} = -[k_1\cos(\phi_j) + k_2\sin(\phi_j)]$, then the matrix $B_{j,j}$ can be rewritten as

$$\begin{aligned} B_{j,j} &= \frac{\exp(i\gamma\Delta t Q_{j,j}) - 1}{i\gamma Q_{j,j}} \cdot \frac{\exp(-\frac{i}{2}\gamma\Delta t Q_{j,j})}{\exp(-\frac{i}{2}\gamma\Delta t Q_{j,j})} \\ &= \Delta t \operatorname{sinc}\left(\frac{1}{2}\gamma\Delta t Q_{j,j}\right) \exp\left(\frac{i}{2}\gamma\Delta t Q_{j,j}\right) \end{aligned} \quad (3.3.10)$$

with the sinc function

$$\begin{aligned} \operatorname{sinc}\left(\frac{1}{2}\gamma\Delta t Q_{j,j}\right) &= \frac{\sin(\frac{1}{2}\gamma\Delta t Q_{j,j})}{\frac{1}{2}\gamma\Delta t Q_{j,j}} \\ &= \frac{\exp\left(\frac{i}{2}\gamma\Delta t Q_{j,j}\right) - \exp\left(-\frac{i}{2}\gamma\Delta t Q_{j,j}\right)}{i\gamma\Delta t Q_{j,j}} \end{aligned} \quad (3.3.11)$$

Then finally, we can find the density function in Fourier space $\hat{u}_{k_1,k_2}(t + \Delta t)$ by

$$\hat{u}_{\phi,k_1,k_2}(t + \Delta t) \approx A\hat{u}_{\phi,k_1,k_2}(t) + B\hat{N}_{\phi,k_1,k_2}(t) \quad (3.3.12)$$

Finally, the density function at new time step $u(\phi, x_1, x_2, t + \Delta t)$ can be calculated by Inverse Fourier Transform

$$u(\phi, x_1, x_2, t + \Delta t) = \frac{1}{N^2} \sum_{k_1=-\frac{N}{2}}^{\frac{N}{2}} \sum_{k_2=-\frac{N}{2}}^{\frac{N}{2}} \hat{u}_{k_1,k_2}(\phi, t) \exp\left(i[k_1x_1 + k_2x_2]\right) \quad (3.3.13)$$

3.4 Calculating the Interaction Term

As indicated in the last section, the interaction term is

$$N(u(t), t) = -\lambda'(\phi, x_1, x_2)u(\phi, x_1, x_2, t) + \int_{\phi'=-\pi}^{\pi} S(T(\phi, \phi', x_1, x_2)) u(\phi', x_1, x_2, t) d\phi' \quad (3.4.1)$$

with

$$\begin{aligned} T_j(\phi, \phi', X) &= q_j \int_{\mathbb{R}^2} K_j^d(X - S) K_j^o(\phi, X - S) w_j(\phi, \phi', X - S) U(S, t) dS \\ \lambda_j(\phi, X) &= \int_{-\pi}^{\pi} T_j(\phi, \phi', X) d\phi \end{aligned} \quad (3.4.2)$$

Then the system can be simplified as

$$\partial_t u(\phi, X, t) + \gamma e_\phi \cdot \nabla_X u(\phi, X, t) = N(u(\phi, X, t)) \quad (3.4.3)$$

with $X \in [-\pi, \pi]^2$. Then if we find a scale for space L_{scale} and time T_{scale} such that $\tilde{X} = L_{scale}(x_1, x_2)$ and $\tilde{t} = T_{scale}(t)$. Then if we substitute the non-dimensionalized variables to (3.4.3), we will get

$$\frac{1}{T_{scale}} \partial_{\tilde{t}} u(\phi, \tilde{X}, \tilde{t}) + \frac{\gamma}{L_{scale}} e_\phi \cdot \nabla_{\tilde{X}} u(\phi, \tilde{X}, \tilde{t}) = N(u(\phi, \tilde{X}, \tilde{t})) \quad (3.4.4)$$

To simplify the function, we can choose $T_{scale} = \frac{L_{scale}}{\gamma}$ with $L_{scale} = \gamma = 1$. Then, $T_{scale} = 1$ and also there is no need to rescale other parameters.

To compute the Turning function, we need to use the Convolution Theorem.

First, we combine the Kernels $K_d(X - S)$, $K_o(X - S, \phi)$ and the probability function $w_j(\phi, \phi', X - S)$ to form a new term $Kw_j(\phi, \phi', X - S)$ which does not

change over time. The turning function is a convolution over space

$$T_j(\phi, \phi', X) = q_j \int_{\mathbb{R}^2} K w_j(\phi, \phi', X - S) U(S, t) dS \quad (3.4.5)$$

Then, we can apply the Fourier transform over the space term $X = (x_1, x_2)$.

$$\hat{T}_j(\phi, \phi', k_1, k_2) = \int_{\mathbb{R}^2} T_j(\phi, \phi', x_1, x_2) \exp(-ix_1 k_1 - ix_2 k_2) dx_1 dx_2 \quad (3.4.6)$$

where k_1, k_2 are the wave numbers. Let $p_1 = x_1 - s_1, p_2 = x_2 - s_2, q_1 = s_1, q_2 = s_2$, then $x_1 = p_1 + q_1, x_2 = p_2 + q_2$

$$\begin{aligned} \hat{T}_j(\phi, \phi', k_1, k_2) &= q_j \int_{\mathbb{R}^2} \int_{\mathbb{R}^2} K w_j(\phi, \phi', p_1, p_2) U(q_1, q_2, t) dq_1 dq_2 \exp(-ix_1 k_1 - ix_2 k_2) dx_1 dx_2 \\ &= q_j \int_{\mathbb{R}^2} \int_{\mathbb{R}^2} K w_j(\phi, \phi', p_1, p_2) U(q_1, q_2, t) \exp(-i(q_1 + p_1)k_1 - i(q_2 + p_2)k_2) dq_1 dq_2 dp_1 dp_2 \\ &= q_j \int_{\mathbb{R}^2} U(q_1, q_2, t) \exp(-iq_1 k_1 - iq_2 k_2) dq_1 dq_2 \int_{\mathbb{R}^2} K w_j(\phi, \phi', p_1, p_2) \exp(-ip_1 k_1 - ip_2 k_2) dp_1 dp_2 \\ &= q_j \widehat{K w_j}(\phi, \phi', k_1, k_2) \hat{U}(k_1, k_2, t) \end{aligned} \quad (3.4.7)$$

Then we can use inverse Fourier transform to find Turning function

$$T_j(\phi, \phi', x_1, x_2) = \int_{\mathbb{R}^2} \hat{T}_j(\phi, \phi', k_1, k_2) \exp(ix_1 k_1 + ix_2 k_2) dk_1 dk_2 \quad (3.4.8)$$

With known turning function, the saturation function can be applied and finally, calculate the interaction term with the most updated density $u(\phi, \phi', X, t)$.

With the turning function calculated in the real space, we can apply our saturation function $S(T)$ to the it. Then for the moving in term, we can combine

the saturated turning term with the density term

$$Su_j(\phi, \phi', x_1, x_2) = S(T(\phi, \phi', x_1, x_2)) u(\phi', x_1, x_2, t) \quad (3.4.9)$$

If we take the Fourier transform in the angle ϕ' , with corresponding wave number k_3 , we get

$$\widehat{Su}_j(\phi, k_3, X) = \alpha \int_{\phi'=-\pi}^{\pi} Su_j(\phi, \phi', X) \exp(-ik_3\phi') d\phi' \quad (3.4.10)$$

Thus we can compute the integral over ϕ' by compute the Fast Fourier Transform over the term ϕ' , and then the integral is equal to the Fourier transform of Su_j when wave number $k_3 = 0$ with normalization term α .

$$\int_{\phi'=-\pi}^{\pi} Su_j(\phi, \phi', X) d\phi' = \alpha \widehat{Su}_j(\phi, 0, X) \quad (3.4.11)$$

Similarly, we can calculate the moving out term $\lambda'_j(\phi, X)$ by

$$\lambda'_j(\phi, X) = \alpha \widehat{S(T)}(0, \phi', X) \quad (3.4.12)$$

where $\widehat{S(T)}(0, \phi', X)$ is the Fourier transform of the function $S(T)(0, \phi', X)$ over then angle space ϕ .

Chapter 4

Results

In this section, we are going to show the results with the saturated interaction term. There are a total of two initial cases we have tested on. The first one is one single Gaussian bump in the center and the other one is two Gaussian bumps. Also, different saturation functions are applied to different initial conditions. The plots shown are the total density $U(x_1, x_2, t)$, which is calculated by

$U(x_1, x_2, t) = \frac{2\pi}{N} \sum_{\phi_j=0}^{j=64} u(\phi_j, x_1, x_2, t)$ where $N = 64$ is the number of grid points during the simulation. The reason to choose $N = 64$ is for balancing the efficiency and accuracy of the implementation. For the time step value dt , we let $dt = 0.01$ in consideration of stability and efficiency throughout the tests. Please check Appendix B for the convergence test and asymmetry test of the ETD scheme.

The videos about the dynamics of the aggregation model are referred in Appendix C. When saturation function is applied, the histograms of the values of turning functions are demonstrated in Appendix A. In each histogram, there is a peak of the occurrences of very small turning rate. This is actually the turning rate at the positions where there is no change of the density within the distance

kernels at certain positions. During the analysis, we would focus on the turning rate with a greater magnitude and how it would be affected by the application of different saturation functions.

4.1 Initial condition 1: One Gaussian bump

The first initial condition is only one Gaussian bump at the center, and the rest area has an evenly distributed density

$$u_0(\phi, X) = \begin{cases} 10000 \cdot \exp(-(x_1^2 + x_2^2)) & \phi = -\pi, 0 \\ 100 & \text{otherwise} \end{cases} \quad (4.1.1)$$

If there is no interaction term in effect, the model is linear and the Gaussian bump is moving constantly toward the angle ϕ at speed $\gamma = 1$, as shown in Figure 4.1.

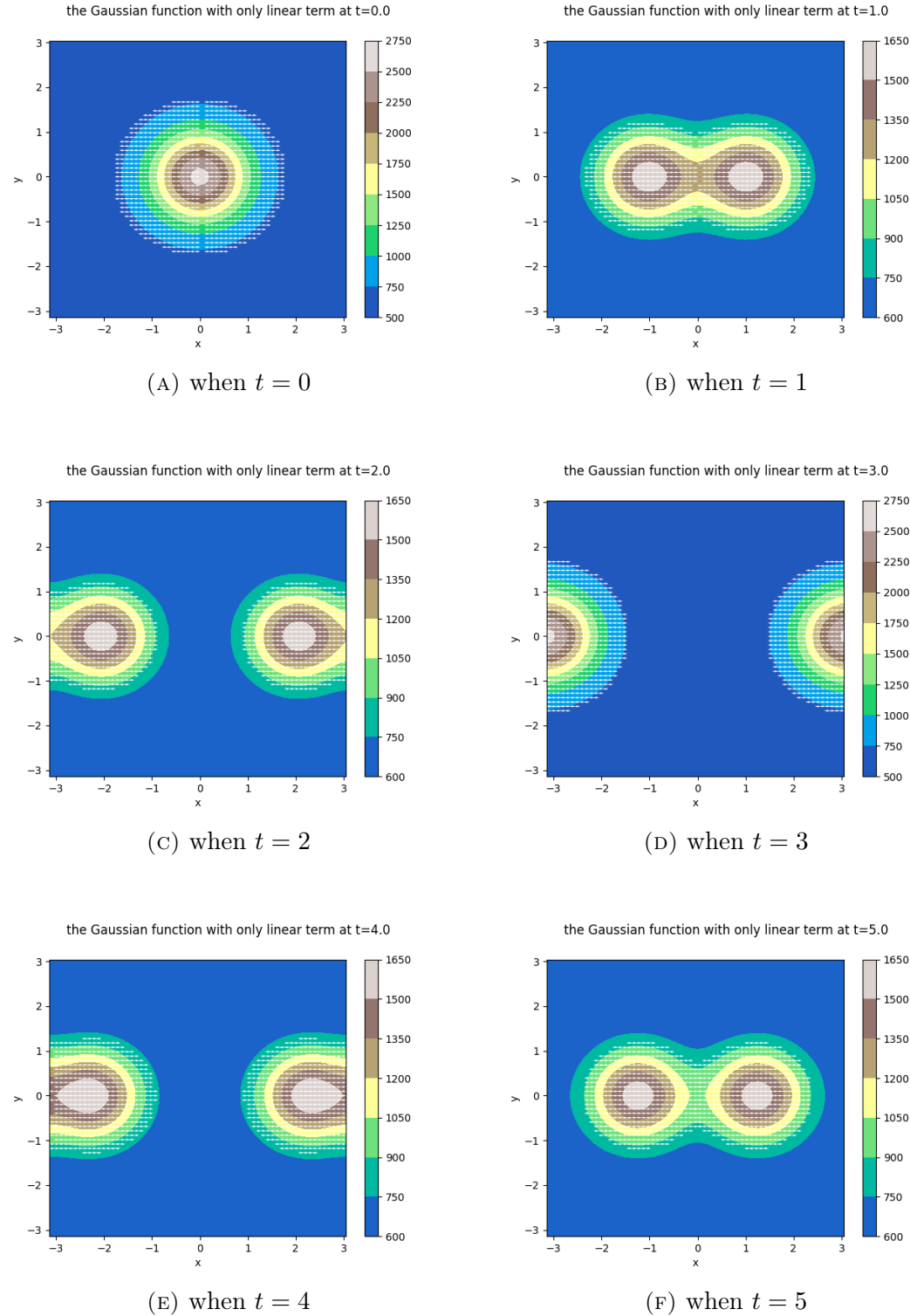


FIGURE 4.1: the Total Population Density $U(x_1, x_2, t)$ of the model with initial condition (4.1.1) when only transportation term is in effect at $t = 0, 0.5, 1.0, 1.5, 2.0$ and 2.5 . The arrows represent the angles with the highest density at the position (x_1, x_2) .

Then, the interaction term is added to the model. For the interaction parameters, we set attraction to be dominant, where $q_a = 2$, $m_a = 0.3$, $d_a = 0.5$; for the repulsive kernels, we set $q_r = 0.5$, $m_r = 0.2$, $d_r = 0$. For the probability function w , we set the width to be $\sigma = 1$ and $|\kappa_j| = 1$. If there is no saturation function applied to the model, the system behaviour is shown in Figure 4.2. From the figures, the two groups moving in opposite directions start to interact with each other by changing their directions, which leading to a disperse in all directions from the center bump.

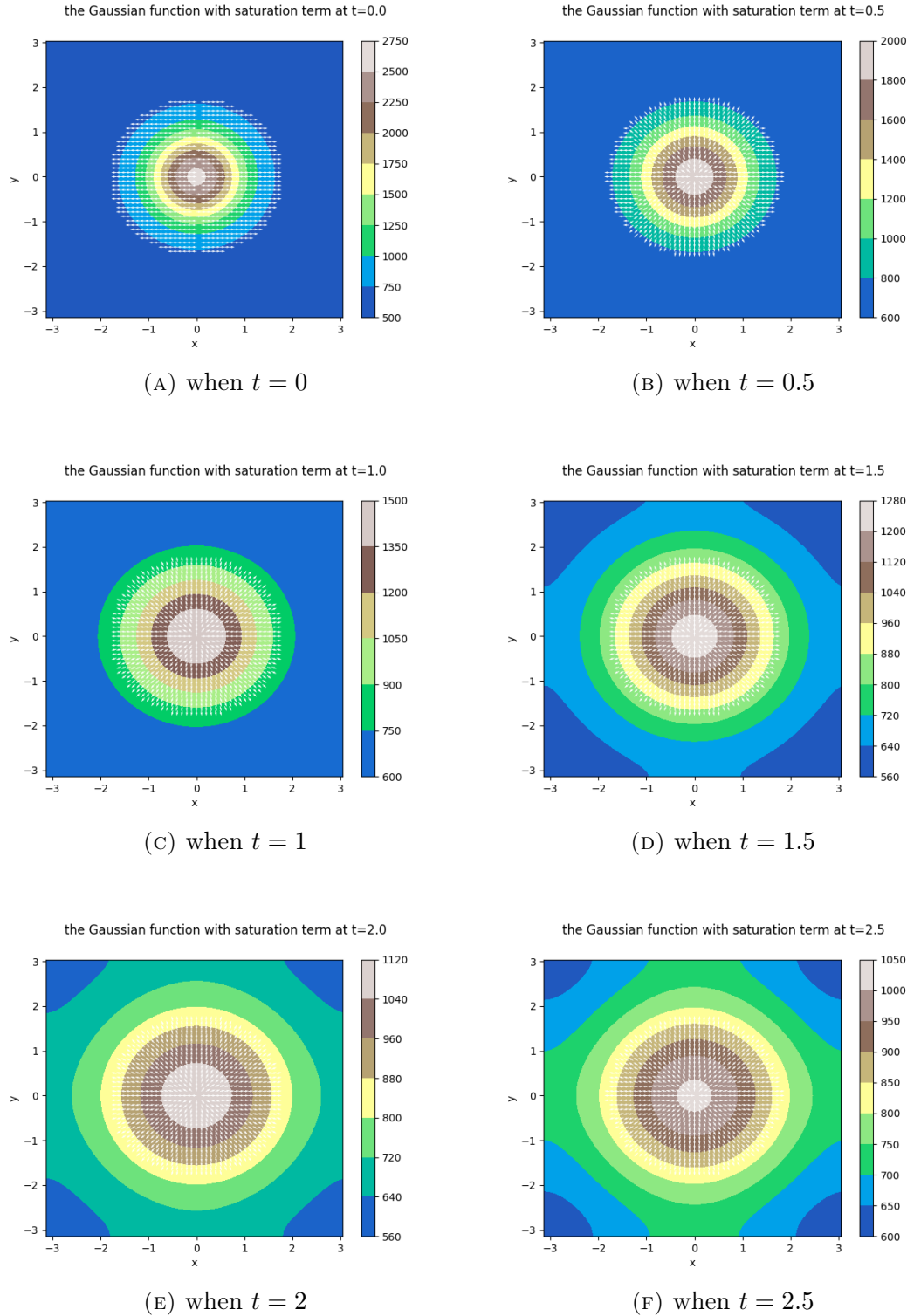


FIGURE 4.2: the Total Population Density $U(x_1, x_2, t)$ when no saturation function is applied to the turning function with $q_a = 2, q_r = 0.5$ of the model with initial condition (4.1.1) at $t = 0, 0.5, 1.0, 1.5, 2.0$ and 2.5 . The arrows represent the angles with the highest density at the position (x_1, x_2) .

Then we apply the saturation function to the interaction term. In this case, we applied

$$S(T) = \frac{5}{2}(1 + \tanh(\frac{T - 5}{1.2})) \quad (4.1.2)$$

where the maximum value $H = 5$, and centred at $\mu = 5$ with the width $\sigma = 1.2$.

The plot of the saturation function is shown on Figure 4.3.

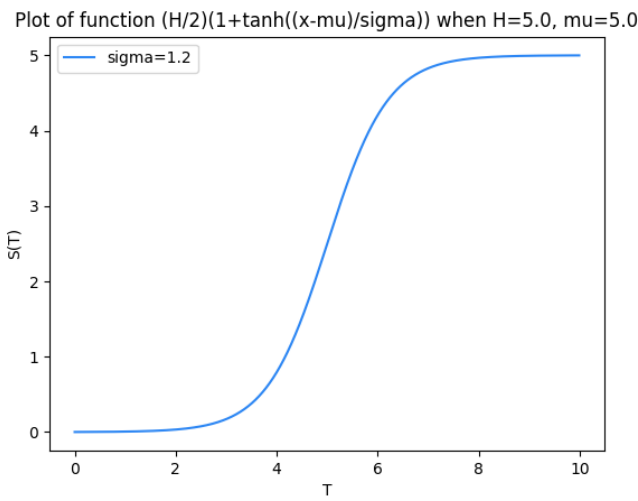


FIGURE 4.3: The Saturation Function (4.1.2) where $H = 5$, $\mu = 5$ and $\sigma = 1.2$.

And then the model with saturated interaction term is shown below. From the figures, we can see that at the beginning when t is small, many individuals are interacting with their neighbours and change their directions. But as t increased, the effect of the interaction term starts to decrease due to the effect of the saturation term. As shown in the histograms in Figure A.1, when $t = 0$, there is a long tail where $T(\phi, \phi', X) > 4$. By applying the saturation function (4.1.2), these turning rates are not completely suppressed but are adjusted to $T(\phi, \phi', X) = 5$. When $t = 2.5$, the turning rates are all suppressed by the saturation function to a

value near 0. Therefore, the transportation term starts to dominate the model and the interaction between the individuals are decreased.

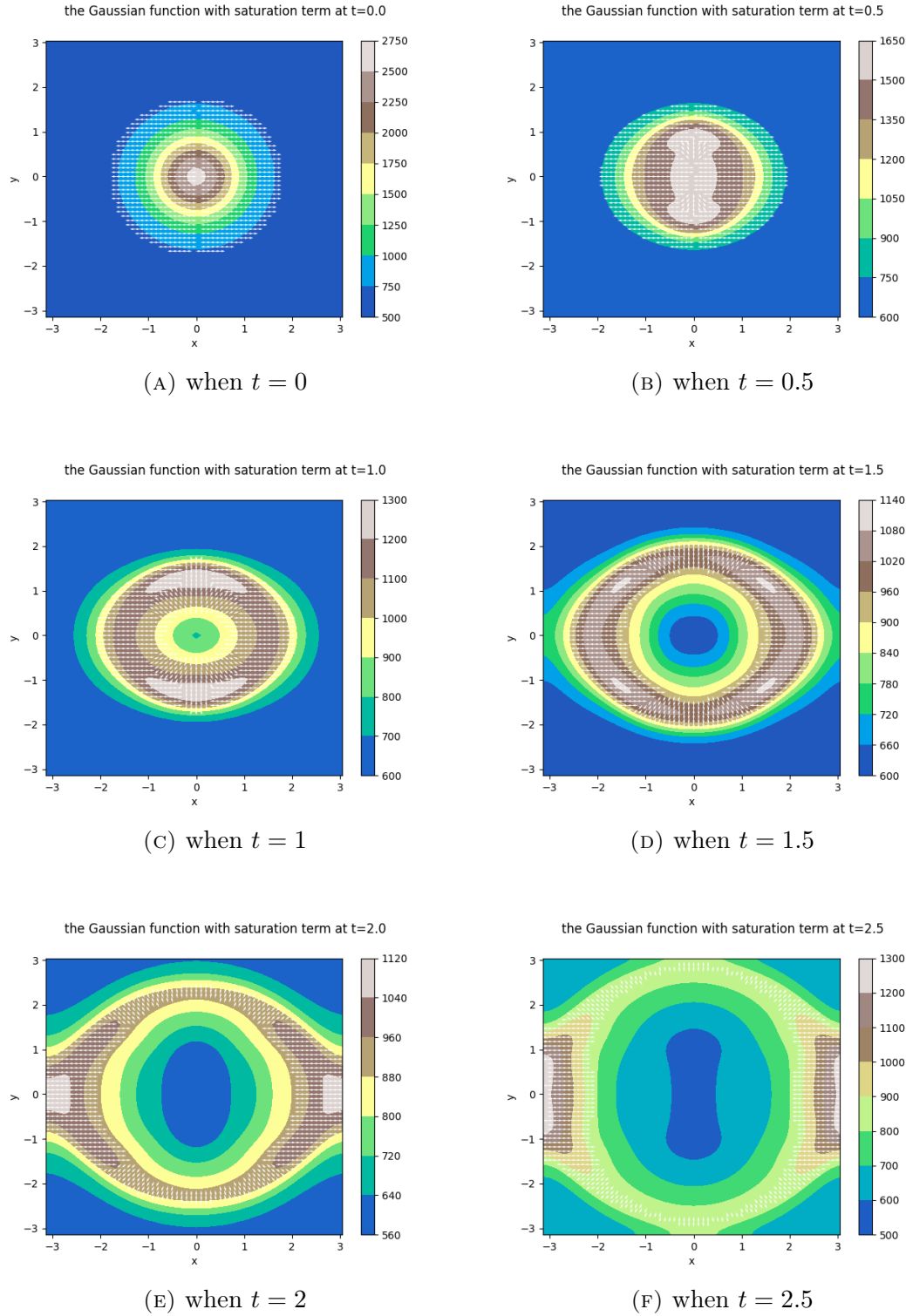


FIGURE 4.4: the Total Population Density $U(x_1, x_2, t)$ when saturation function (4.1.2) is applied to the turning function with $q_a = 2, q_r = 0.5$ of the model with initial condition (4.1.1) at $t = 0, 0.5, 1.0, 1.5, 2.0$ and 2.5 . The arrows represent the angles with the highest density at the position (x_1, x_2) .

4.2 Initial condition 2: Two Gaussian bumps

In this section, the initial condition has two Gaussian bumps with different mass at each bump, where

$$u_0(\phi, X) = \begin{cases} 10000 \cdot \exp(-(10 \cdot ((x_2 + 0.5)^2 + x_1^2))) & \phi = -\frac{\pi}{2} \\ 5000 \cdot \exp(-(10 \cdot ((x_1 + 0.5)^2 + x_2^2))) & \phi = -\pi \\ 100 & \text{otherwise} \end{cases} \quad (4.2.1)$$

For the interaction parameters, we set the values to be the same as the previous example. We first run the model without any saturation function. From Figure 4.5, we can see that at first, the repulsion term is dominant and the two bumps started to spread out at different angles. However, as time increases, although the bumps keep spreading out, there is still an attraction force between the individuals such that they finally form one big bump instead of two bumps at the beginning.

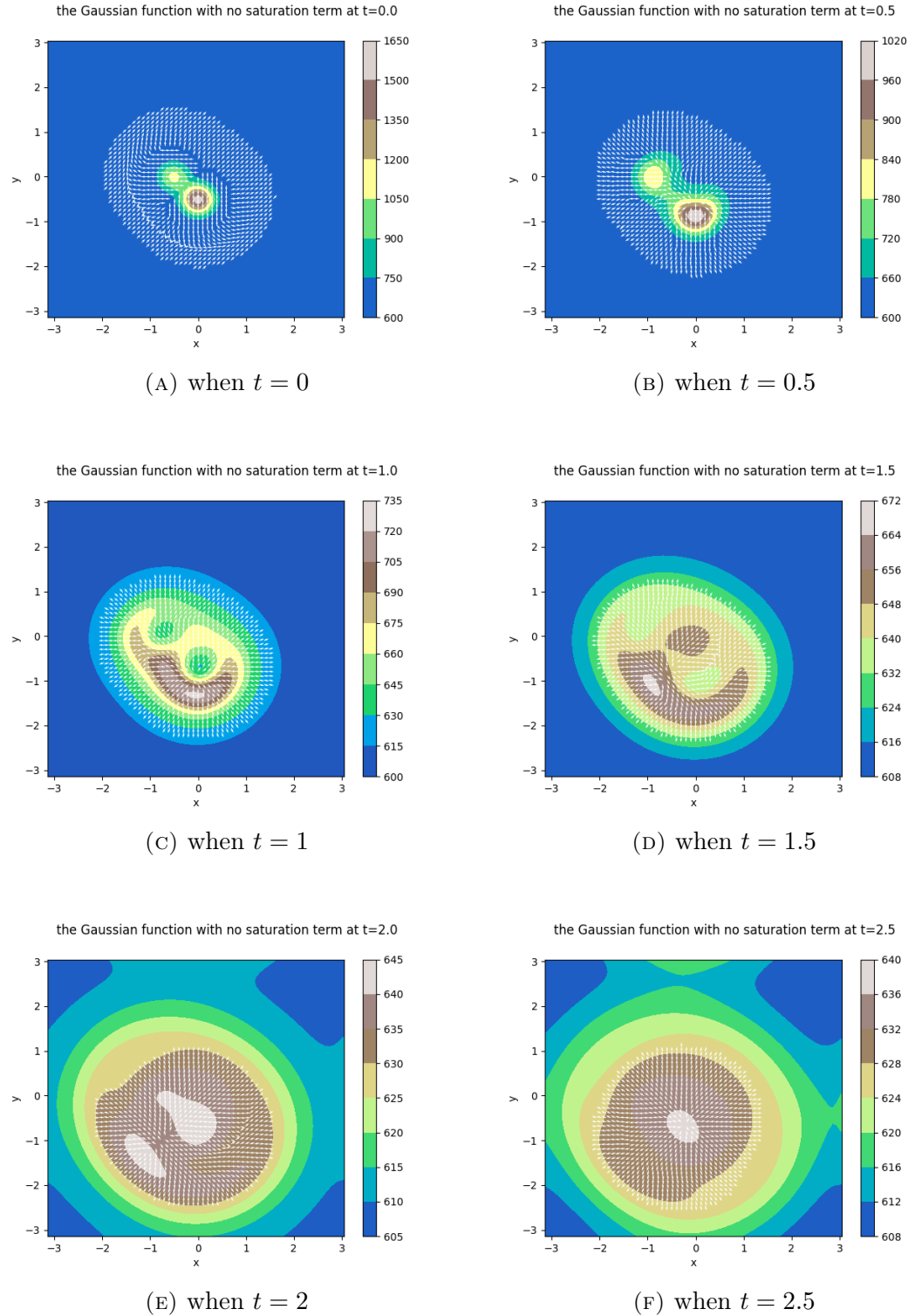


FIGURE 4.5: the Total Population Density $U(x_1, x_2, t)$ when no saturation function is applied to the turning function with $q_a = 2, q_r = 0.5$ of the model with initial condition (4.2.1) at $t = 0, 0.5, 1.0, 1.5, 2.0$ and 2.5 . The arrows represent the angles with the highest density at the position (x_1, x_2) .

Now if we apply the same saturation function in (4.1.2), the result shows in Figure 4.6, which seems like there is only the transportation term in effect with very little repulsive interaction force. The reason is that for this initial condition, the range of the turning function is [0, 3.59], as shown in Figure A.3. When we apply saturation function (4.1.2), most of the turning function values are in the minimum section and finally transform into values very close to zero.

If we would like to establish a model with a similar behaviour shown in Figure 4.4 where the interaction between the individuals are not completely suppressed, we can apply another saturation function such that the turning function still affects the model to interact with its neighbours.

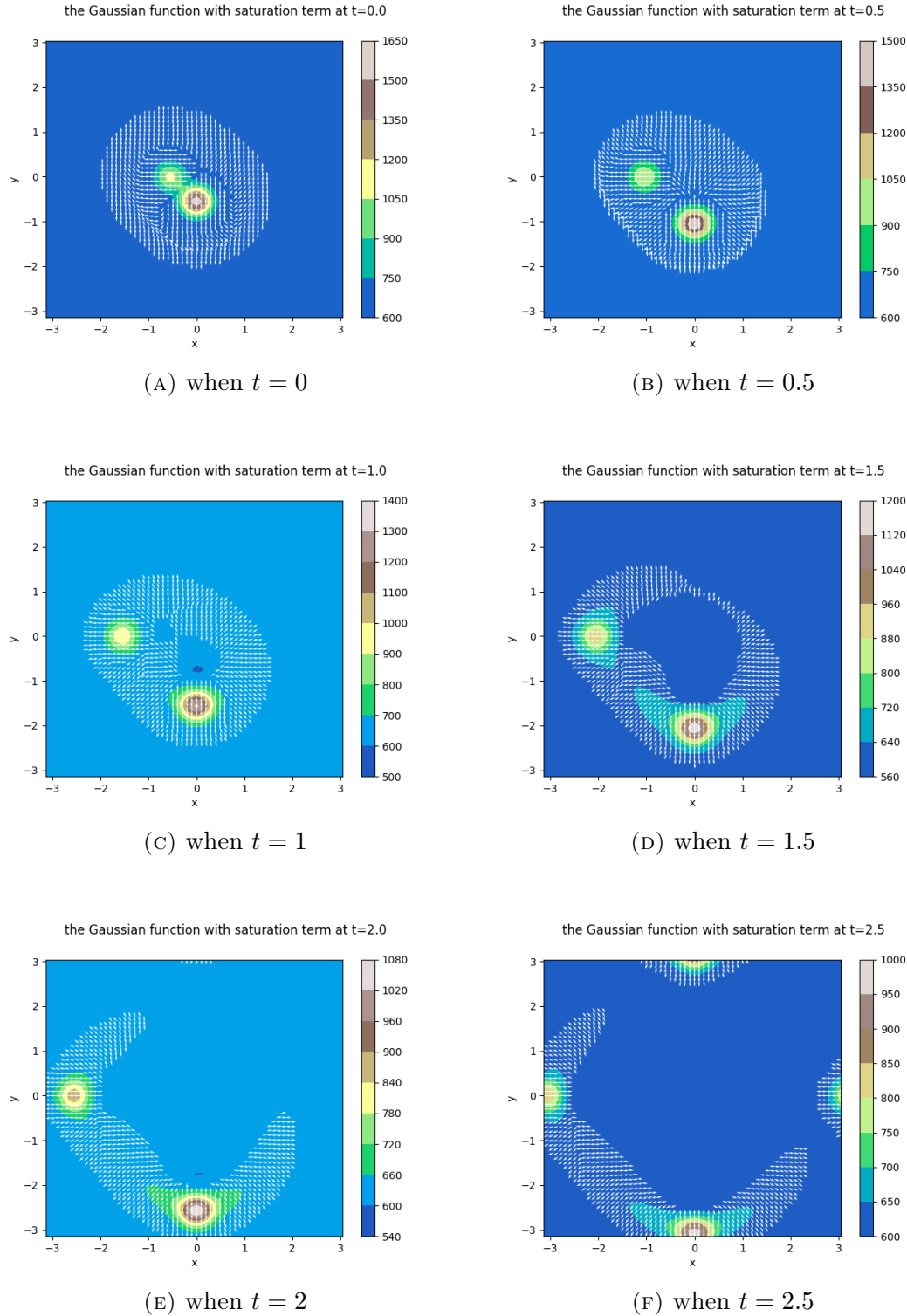


FIGURE 4.6: the Total Population Density $U(x_1, x_2, t)$ when saturation function (4.1.2) is applied to the turning function with $q_a = 2, q_r = 0.5$ of the model with initial condition (4.2.1) at $t = 0, 0.5, 1.0, 1.5, 2.0$ and 2.5 . The arrows represent the angles with the highest density at the position (x_1, x_2) .

Therefore, we applied a new saturation function

$$S(T) = \frac{2}{2}(1 + \tanh(\frac{T - 2}{1})) \quad (4.2.2)$$

which shown in Figure 4.7 with $H = 2, \mu = 2$ and $\sigma = 1$.

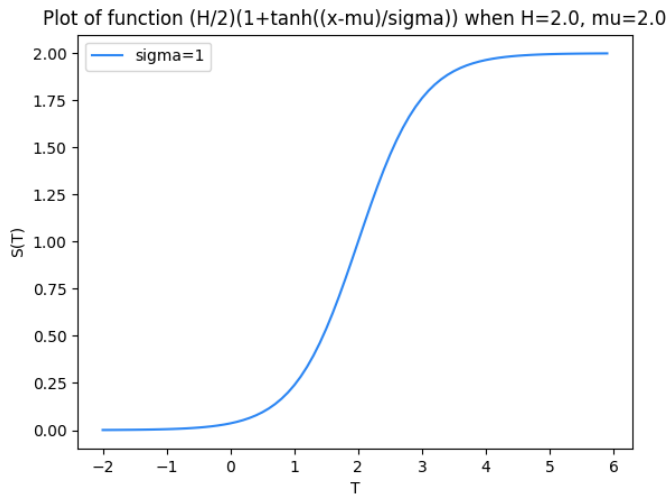


FIGURE 4.7: The Saturation Function (4.2.2) where $H = 2, \mu = 2$ and $\sigma = 1$

By comparing the histograms of the turning rates in Figure A.4 and the saturation function in Figure 4.7, we can see that for most values of the turning function, it falls into the slope section in the saturation function. Also, with some small values of the turning functions, they transform into values close to 0. If we apply the new saturation function (4.2.2) to the model, the result is shown in Figure 4.8. From the plots, we can see that at the beginning, the two bumps are interacting with each other and tending to form one big bump. However, as t increases, the histograms in Figure A.4 show that many values of the turning

function fall into the minimum section of the saturation function. As the result, the individuals stopped interacting with each other but just move in their own directions.

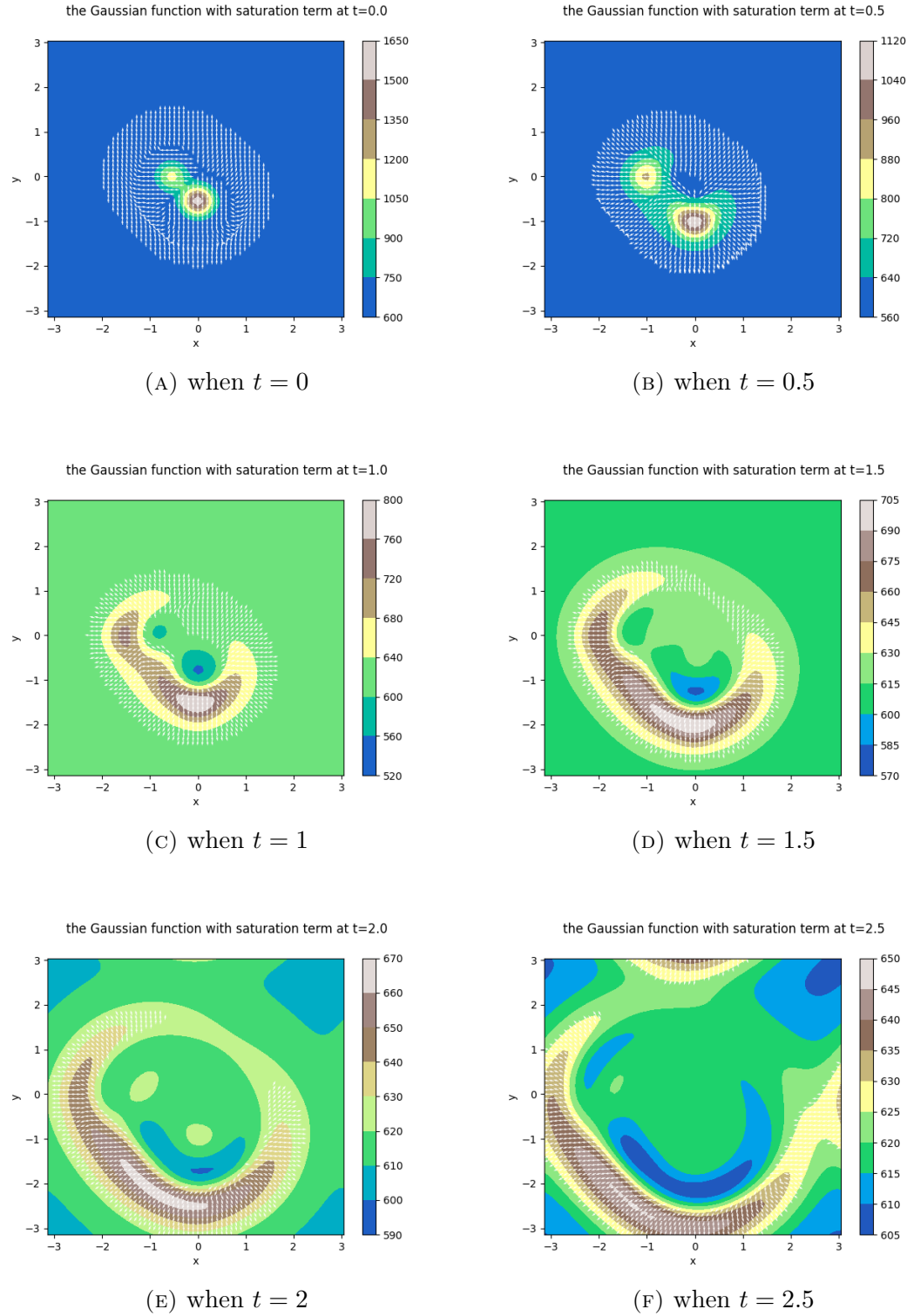


FIGURE 4.8: the Total Population Density $U(x_1, x_2, t)$ when saturation function (4.2.2) is applied to the turning function with $q_a = 2, q_r = 0.5$ of the model with initial condition (4.2.1) at $t = 0, 0.5, 1.0, 1.5, 2.0$ and 2.5 . The arrows represent the angles with the highest density at the position (x_1, x_2) .

Changing the saturation function is not the only way to change the interaction in the system. Similarly, we can change the value of q_a, q_r to simulate the aggregation under different scenarios. In the following test, we set $q_a = 4, q_r = 1$ which is proportional to the original q_a, q_r with the same initial condition. The results shown in Figure 4.9 states that the model starts with a similar spreading out motion as the results in Figure 4.5. Many individuals first change their directions and then start to aggregate and form a big bump between the two bumps. However, since the strength of the interaction forces is increased, the model does not only aggregate faster but also disperses more slowly. This can be shown by comparing Figure 4.5(c),(d) with Figure 4.9(c),(d). In Figure 4.5(c) and (d), there is an aggregation motion but we can still see some unevenly distributed area in the bump. Whereas in Figure 4.9(c) and (d), the model quickly forms a bump similar to a Gaussian bump and disperses more slowly.

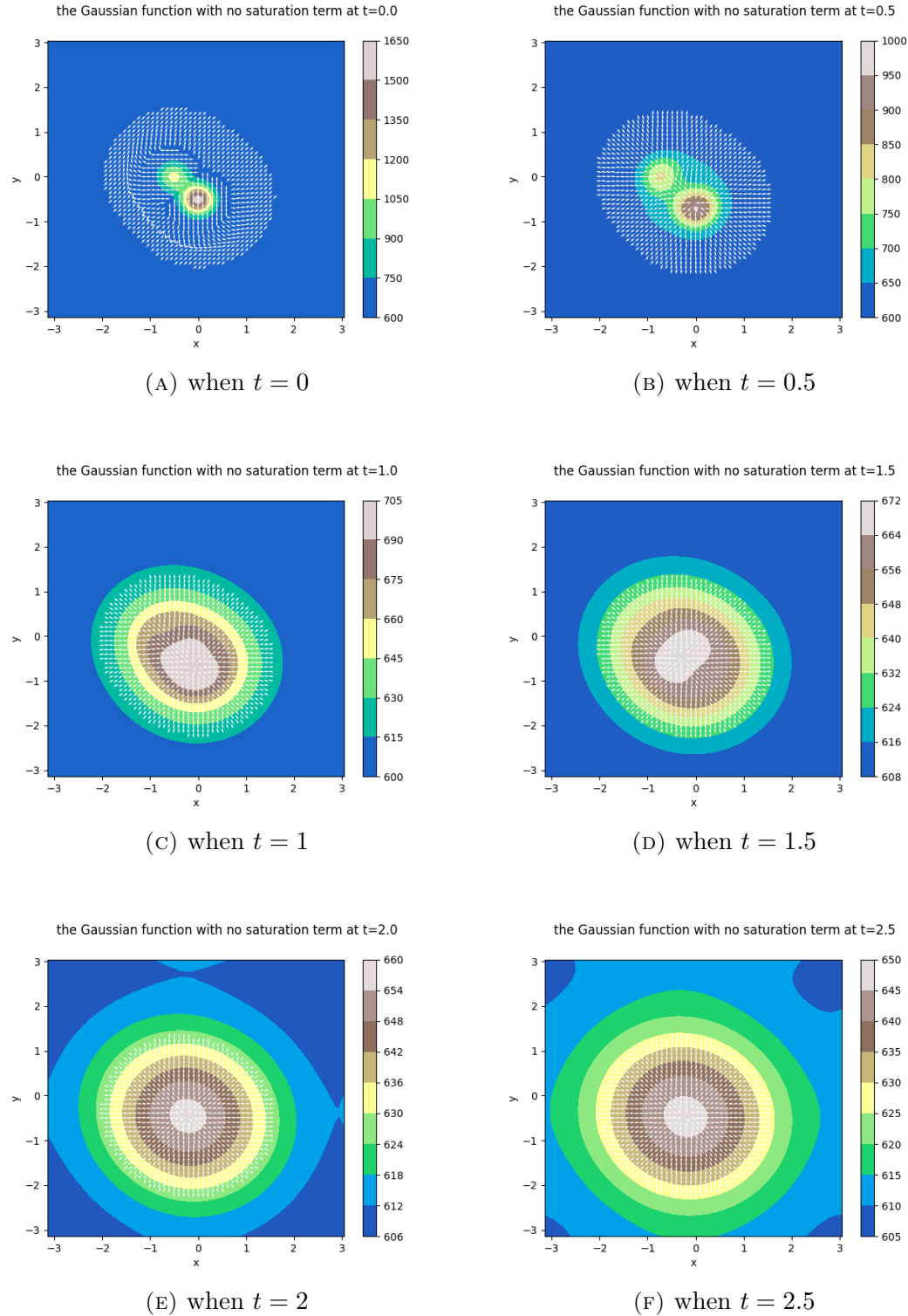


FIGURE 4.9: the Total Population Density $U(x_1, x_2, t)$ when no saturation function is applied to the turning function with $q_a = 4, q_r = 1$ of the model with initial condition (4.2.1) at $t = 0, 0.5, 1.0, 1.5, 2.0$ and 2.5 . The arrows represent the angles with the highest density at the position (x_1, x_2) .

Now if we apply the same saturation function in (4.2.2) to this model, the result is shown in Figure 4.10. From the plots, it is interesting to see that with the saturation term applied, the model behaves similar to the model in Figure 4.5, where no saturation function is applied with smaller q_a, q_r . One important reason is that with the increase of the q_a, q_r , the magnitude of the turning function also increases. In this example, as shown in Figure A.5 the turning function is in the range of $[0, 7.17]$. Therefore, if (4.2.2) is applied, most of the turning function values fall into the maximum section of the saturation function. Then the maximum magnitude of the turning function would be decreased to 2, which is a value closer to the turning function magnitude when $q_a = 2, q_r = 0.5$. Also, since the maximum turning rate equals to 2 when the saturation function (4.2.2) is applied, if we compare Figure 4.10 with Figure 4.9 where the turning function is not saturated, the aggregation between the two bumps becomes much slower.

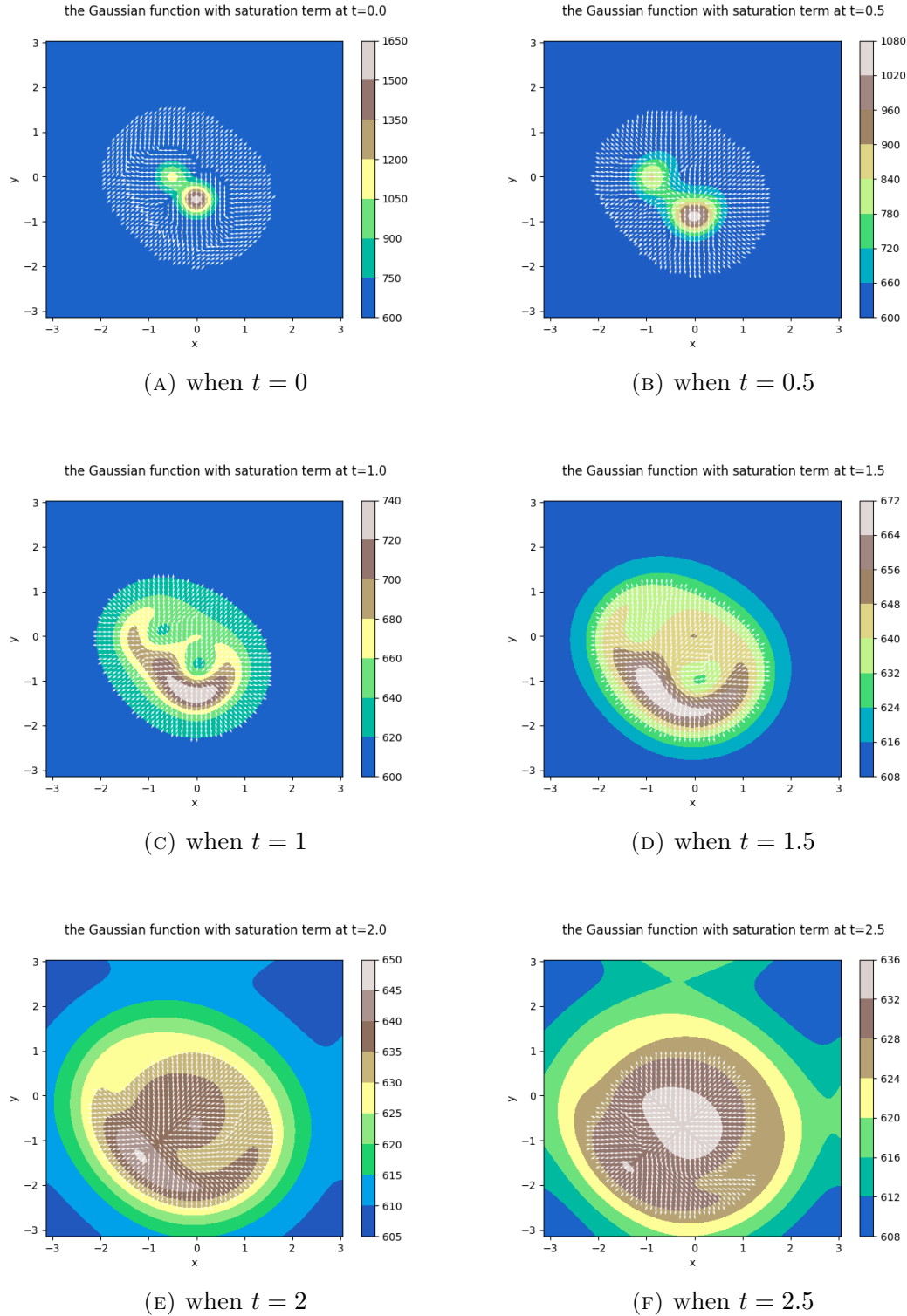


FIGURE 4.10: the Total Population Density $U(x_1, x_2, t)$ when saturation function (4.2.2) is applied to the turning function with $q_a = 4, q_r = 1$ of the model with initial condition (4.2.1) at $t = 0, 0.5, 1.0, 1.5, 2.0$ and 2.5 . The arrows represent the angles with the highest density at the position (x_1, x_2) .

However, if we compare Figure 4.10 and Figure 4.8, where both cases have the same saturation function and initial function applied, the outcome is distinct. In Figure 4.10, the interaction term still has relatively significant influences on the model as t increases, but in Figure 4.8, especially in subplots (e) and (f), the influence of the interaction term has been largely decreased and the transportation term has the main effects on the model. The main reason is that for the case shown in Figure 4.10, at $t = 2$ and $t = 2.5$ in Figure A.5, the maximum of the turning function magnitude is still greater than 2. Therefore, we can apply another saturation function (4.2.3) to the model such that when the values of the turning function decrease, they will be transformed into values closer to 0 by the saturation function.

$$S(T) = \frac{6}{2} \left(1 + \tanh\left(\frac{T - 6}{1}\right)\right) \quad (4.2.3)$$

where $H = 6$, $\mu = 6$ and $\sigma = 1$ with the plot shown in Figure 4.11.

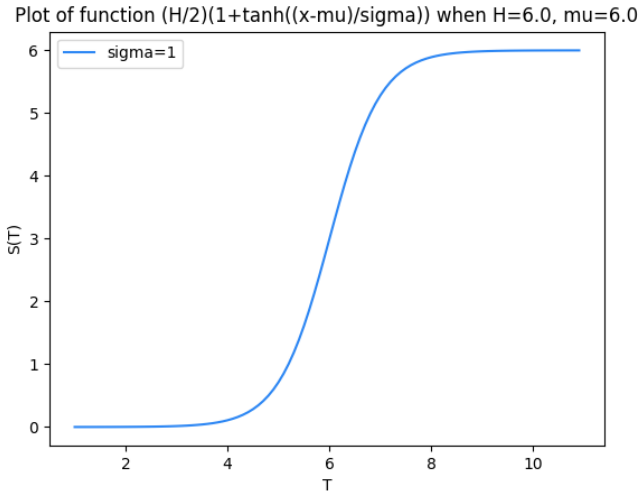


FIGURE 4.11: The Saturation Function (4.2.3) where $H = 6$, $\mu = 6$ and $\sigma = 1$

In Figure 4.12, we can see that in subfigure (a), (b) and (c), there is still some interaction between the two bumps, but as t increases, the interaction force decreases and the transportation term starts to dominate the motion. This behaviour is similar to Figure 4.8 but with different saturation functions applied due to different interaction force strengths.

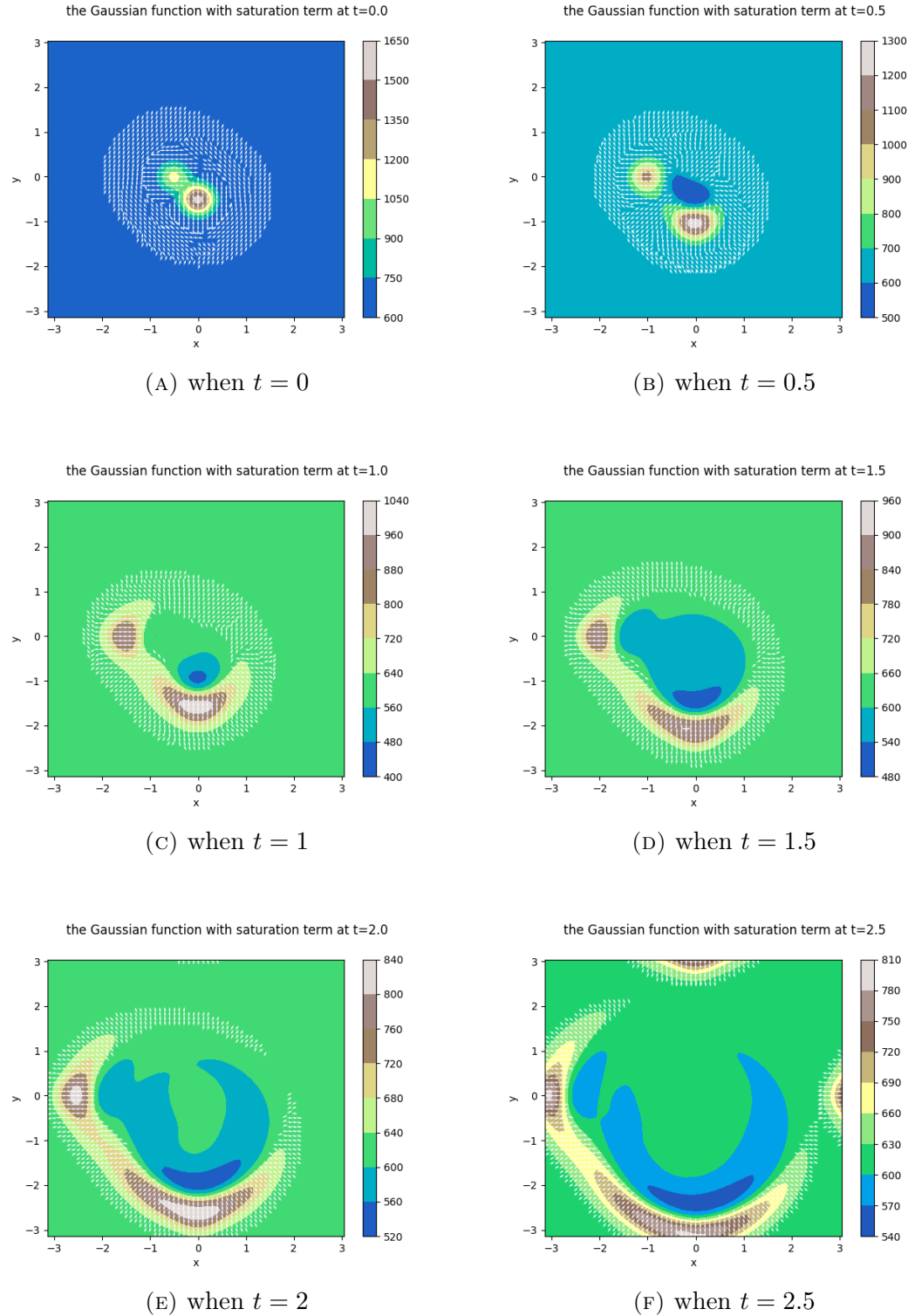


FIGURE 4.12: the Total Population Density $U(x_1, x_2, t)$ when saturation function (4.2.3) is applied to the turning function with $q_a = 4, q_r = 1$ of the model with initial condition (4.2.1) at $t = 0, 0.5, 1.0, 1.5, 2.0$ and 2.5 . The arrows represent the angles with the highest density at the position (x_1, x_2) .

We can also apply another saturation function to the system with the same value of $H = 6$ and $\mu = 6$, but different width $\sigma = 2.5$.

$$S(T) = \frac{6}{2}(1 + \tanh(\frac{T - 6}{2.5})) \quad (4.2.4)$$

As shown in Figure 4.13, the slope section is less steep than the previous saturation function in (4.2.3).

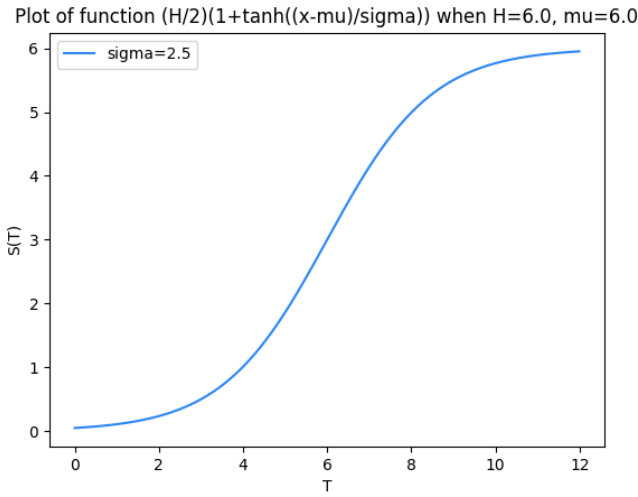


FIGURE 4.13: The Saturation Function (4.2.4) where $H = 6$, $\mu = 6$ and $\sigma = 2.5$

As the new saturation function is applied to the model as shown in Figure 4.14, it demonstrates that as t increases, although the transportation term dominates the model, the interaction forces still have some observable influences on the model.

In the subplot (e) and (f), it forms one peak between the original two bumps whereas, in Figure 4.12, there are always two peaks at $-\pi$ and $-\frac{\pi}{2}$ direction. The main reason is that since the width σ in (4.2.4) is greater than the σ in (4.2.3),

then the minimum section of the saturation function is thinner. If we compare the saturation function in Figure 4.13 with the histograms in Figure A.7, less values in the turning function are suppressed to approximately zero. Therefore, as t increases, many saturated magnitudes of the turning function are still greater than zero and some individuals are still interacting with their neighbours.

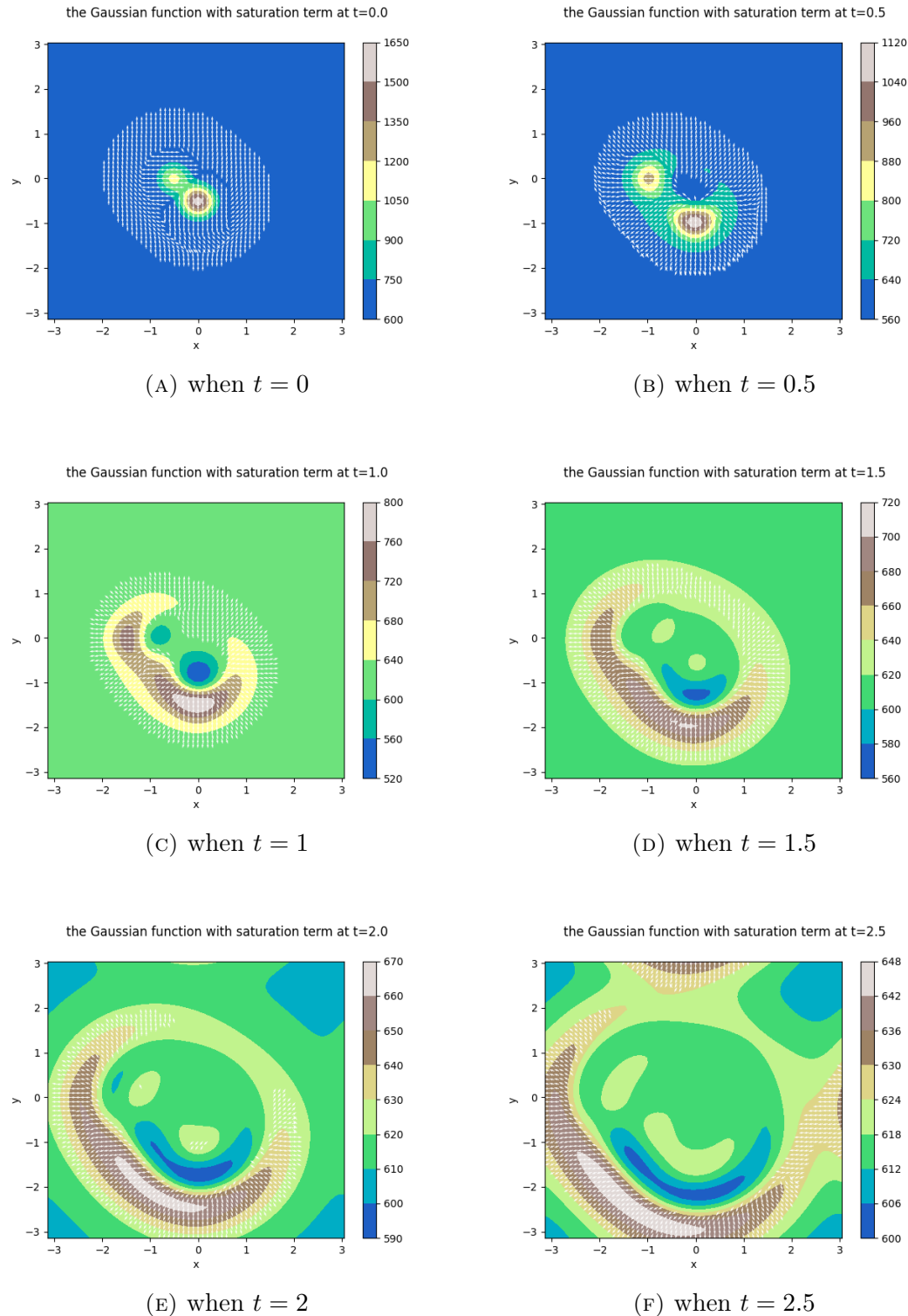


FIGURE 4.14: the Total Population Density $U(x_1, x_2, t)$ when saturation function (4.2.4) is applied to the turning function with $q_a = 4, q_r = 1$ of the model with initial condition (4.2.1) at $t = 0, 0.5, 1.0, 1.5, 2.0$ and 2.5 . The arrows represent the angles with the highest density at the position (x_1, x_2) .

Chapter 5

Conclusions

In a 2+1-dimensional aggregation model, the non-linear interaction part plays a significant role in the behaviour of the aggregation motion. The interaction part mainly states the interaction between the individual and the position of their neighbours for attractive and repulsive motions. In Fetecau's model, they change many different parameters to show the different cases of the aggregation model.

For instance, they had adjusted the κ_j value in the probability function $w_j(\phi, \phi', X - S)$ to change the weight of the kernel for an individual to change from its original orientation ϕ' to a new angle ϕ .

Another way is to directly change the q_j term which represents the strength of attractive or repulsive interaction. In the same system, even if the proportion between q_a and q_r remains the same, the outcome is still different. When the values of q_a and q_r are different, the behaviour of the systems might be similar to each other, but the strength of attractive or repulsive force would vary depending on the value of q_j . If a system is attraction dominated, greater q_j values would result in a faster aggregation behaviour of the model.

In our system, we added another factor, which is the saturation function $S(x)$, to the turning function in the interaction term, to introduce another way to change the behaviour of our model. The saturation function $S(x)$ has three parameters: the maximal height H , the midpoint μ and width σ .

There are three cases that would happen if we add a saturation function to the model, and all three cases are related to the range of turning function values. The first case is when most effectual values of the turning function are placed in the maximum section of the saturation term. Then the system behaviour is highly dependent on the maximum value of the saturation function. The second case is when most of the range of the turning function falls into the minimum section, where most of the turning function values are transferred to values that are really close to zero. In this case, many individuals in the system do not interact with their neighbours but maintain the same angle over time. The third case is when most of the turning function values are in the slope section of the saturation function. In this case, the behaviour of the system would depend on the value of width μ in the saturation function. If μ is relatively small, it means that more turning values would transform into the maximum value H and minimum value 0. If μ becomes larger, then the interaction term will have a greater influence on the model.

The scenarios above can be used to describe different kinds of aggregation motion for many organisms in different environment. Many micro-organisms, such as amoebae (*Dictyostelium discoideum*), are very sensitive to their environment and perform collective movements based on the chemical cues they can detect[11]. Also, when the density of a crowd becomes too high, then the aggregation

movement would stop [1]. In these situations, the adaptation of a saturation function can be used to predict the movement of the total population. Also, with different values of H in the saturation function, it can also amplify or attenuate the interaction between individuals. For instance, some bacteria would be more likely to aggregate and start biofilm formation under stressful survival conditions[5]. In this case, the interaction between individuals can be amplified by applying the saturation function with a relatively greater value of H to simulate the response of bacteria under stress. For this study, there are also some parts that can be further developed. For instance, in some species, there are also alignment interaction force which let each individual to turn to the same angle as their neighbours. In that case, not only the position of the neighbours, but the angles of neighbours would be considered in the system.

The saturation function can also be further developed. In this study, we used hyperbolic tangent function as the saturation function. There are also other increasing and bounded functions which can be applied to the system to simulate other scenarios for the interaction between different organisms.

Bibliography

- [1] G. Courcoubetis et al. “Formation, collective motion, and merging of macroscopic bacterial aggregates”. In: *PLoS Computational Biology* 18(1) (2022), e1009153.
- [2] I.D. Couzin and J. Krause. “Self-organization and collective behavior in vertebrates”. In: *Advances in the Study of Behavior* 32 (2003), pp. 1–75.
- [3] S. M. Cox and P. C. Matthews. “Exponential time differencing for stiff systems”. In: *Journal of Computational Physics* 176 (1995), 430–455.
- [4] F.R. Favreau, A.W. Goldizen, and O. Pays. “Interactions among social monitoring, anti-predator vigilance and group size in eastern grey kangaroos”. In: *Proceedings of the Royal Society B: Biological Sciences* 277 (1690) (2010), pp. 2089–2095.
- [5] I. Grobas, M. Polin, and M. Asally. “Swarming bacteria undergo localized dynamic phase transition to form stress-induced biofilms”. In: *eLife* 10 (2021), e62632.
- [6] J. Krause and Graeme D. Ruxton. *Living in Groups*. Oxford: Oxford University Press, 2002.

- [7] Anne E. Magurran. “The adaptive significance of schooling as an anti-predator defence in fish”. In: *Annales Zoologici Fennici* 27 (1990), pp. 51–66.
- [8] R.C.Fetecau. “Collective behaviour of biological aggregation in two dimensions: A non-local kinetic model”. In: *Mathematical Models and Methods in Applied Sciences* 21 (2011), 1539–1569.
- [9] G. Roberts. “How many birds does it take to put a flock to flight?” In: *Animal Behaviour* 54 (1997), pp. 1517–1522.
- [10] S. J. Simpson, A. R. McCaffery, and B. F. Hägele. “A behavioural analysis of phase change in the desert locust”. In: *Biological Reviews* 74 (1999), 461–480.
- [11] L. Song et al. “Dictyostelium discoideum chemotaxis: threshold for directed motion”. In: *European Journal of Cell Biology* 85(9-10) (2006), 981–989.
- [12] Lloyd N. Trefethen. *Spectral Methods in MATLAB*. Philadelphia, USA: SIAM: Society for Industrial and Applied Mathematics, 2008.
- [13] T. Vicsek et al. “Novel type of phase transition in a system of self-driven particles”. In: *Physical Review Letters* 75(6) (1995), pp. 1226–1229.

Appendix A

Histogram of Turning Functions

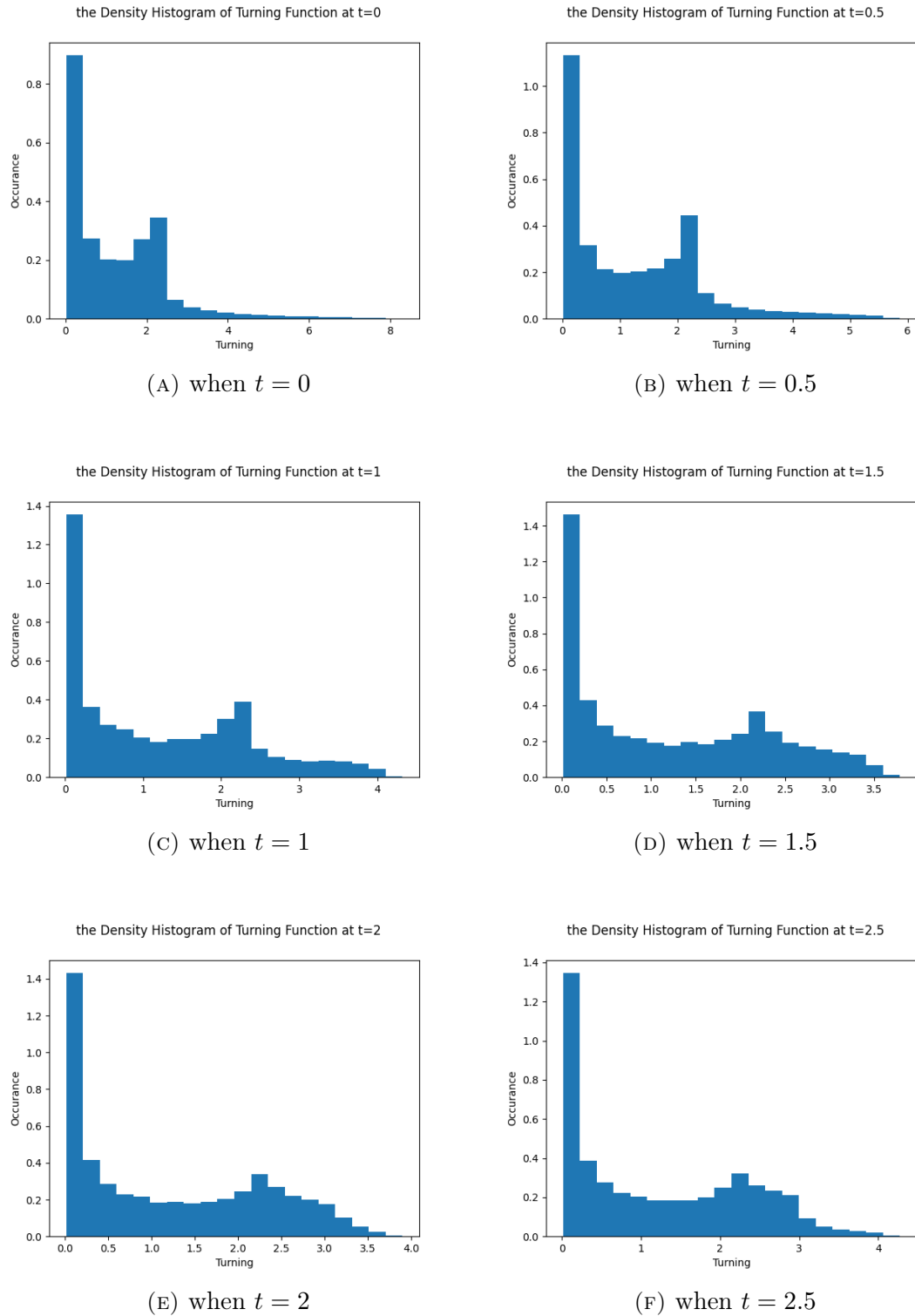


FIGURE A.1: Turning Function Values for Initial Condition (4.1.1)
with saturation function (4.1.2)

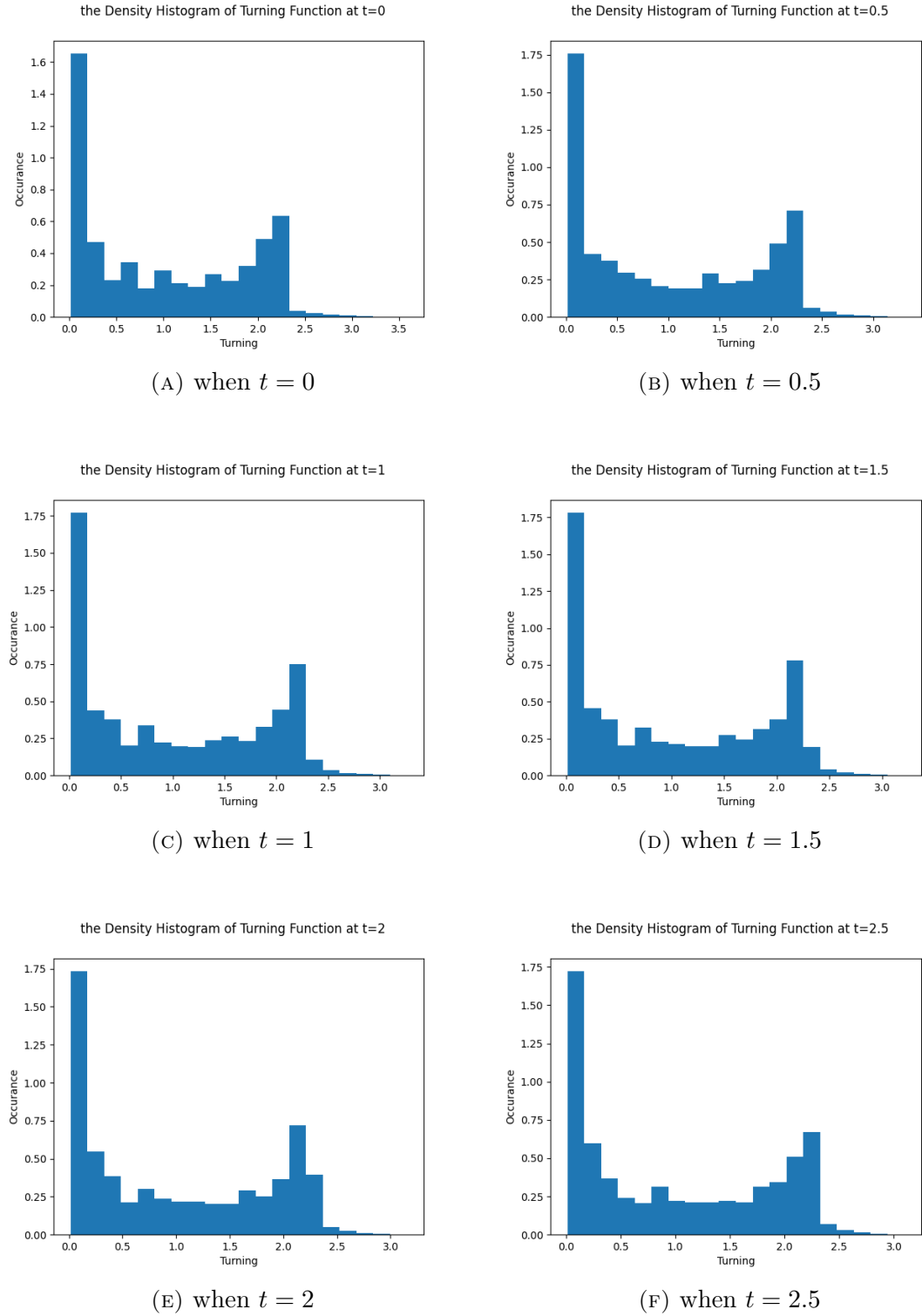


FIGURE A.2: Histogram of Turning Function Values for Initial Condition (4.2.1) with saturation function (4.1.2) when $q_a = 2, q_r = 0.5$

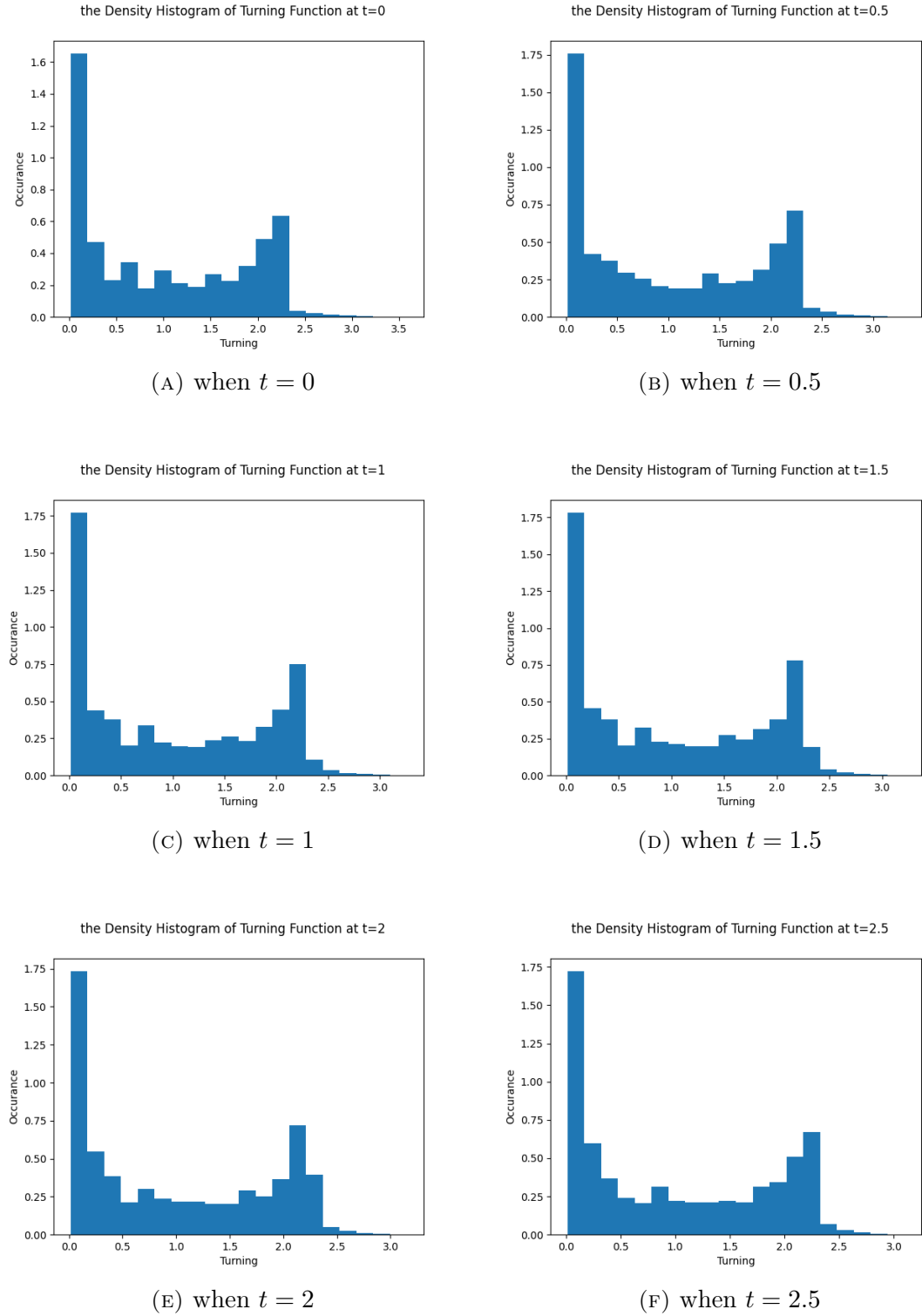


FIGURE A.3: Histogram of Turning Function Values for Initial Condition (4.2.1) with saturation function (4.1.2) when $q_a = 2, q_r = 0.5$

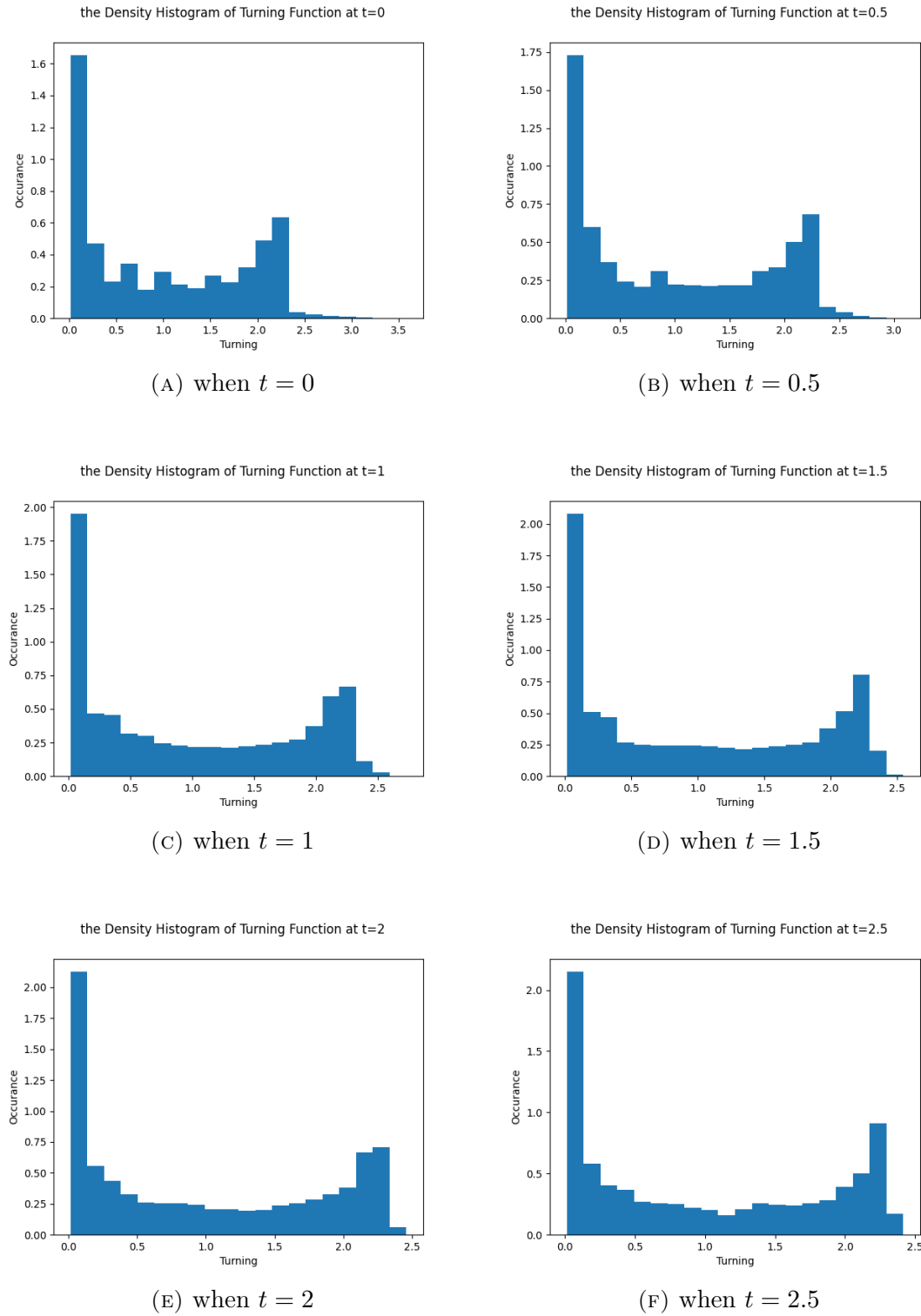


FIGURE A.4: Histogram of Turning Function Values for Initial Condition (4.2.1) with saturation function (4.2.2) when $q_a = 2, q_r = 0.5$

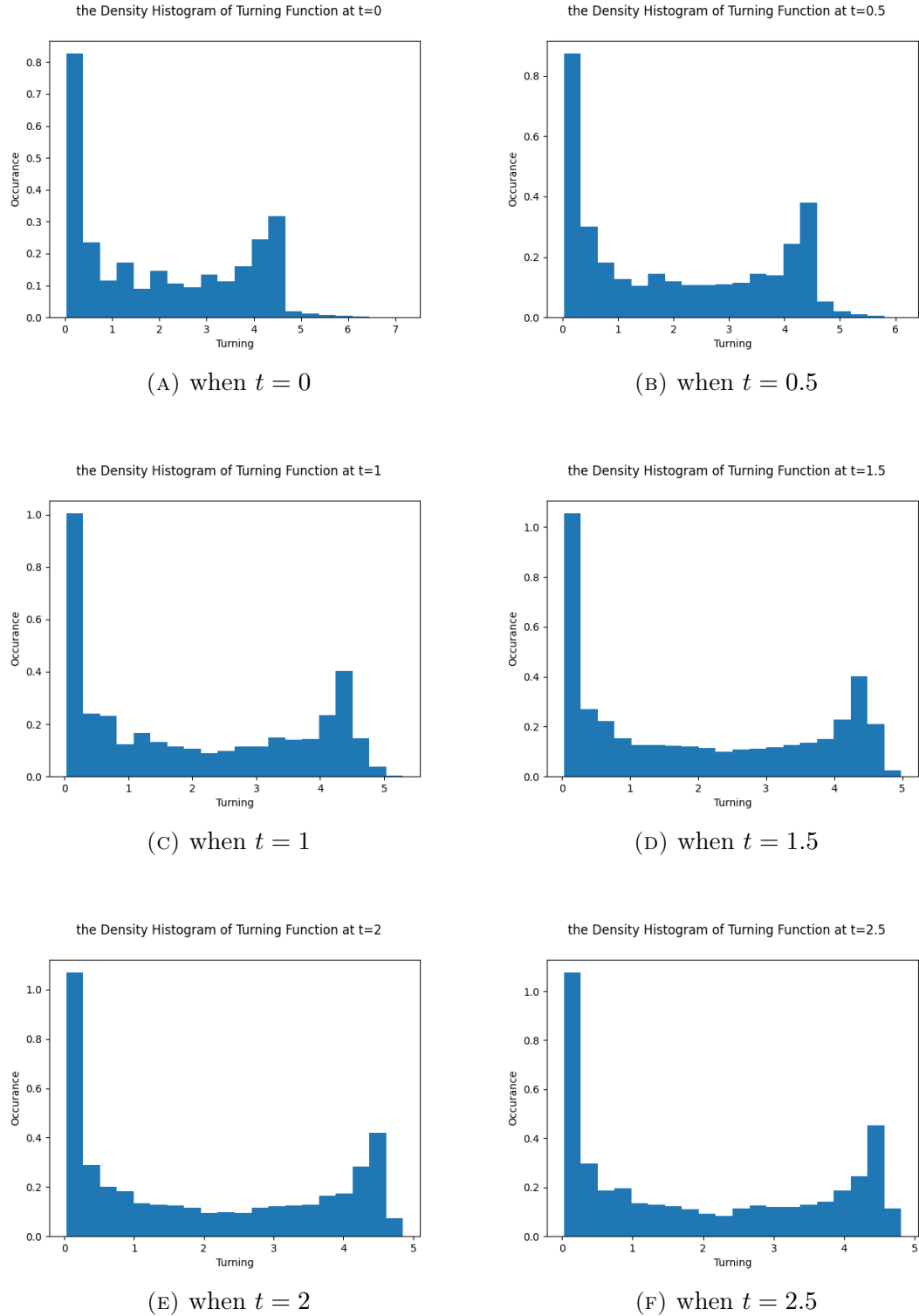


FIGURE A.5: Histogram of Turning Function Values for Initial Condition (4.2.1) with saturation function (4.2.2) when $q_a = 4, q_r = 1$

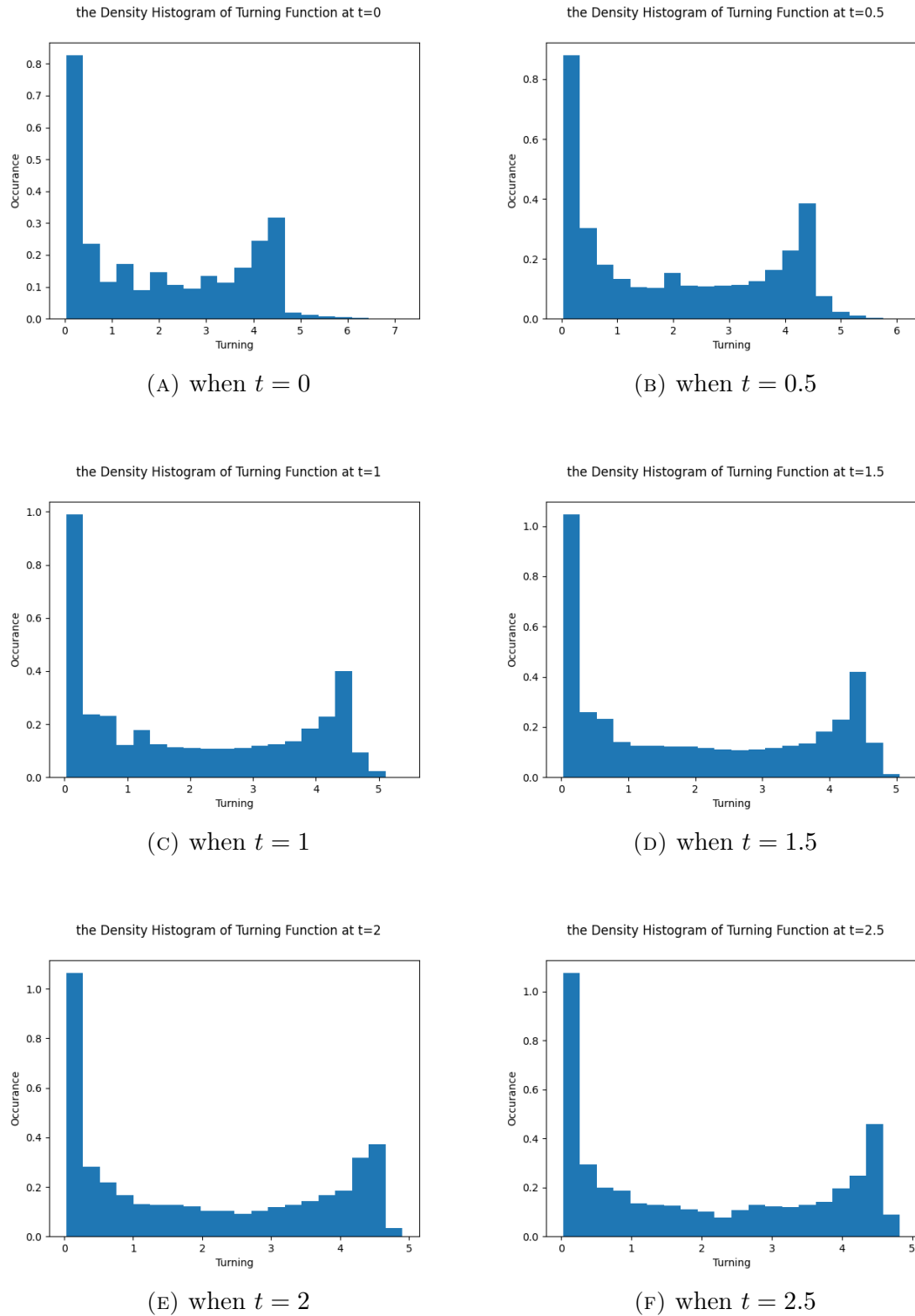


FIGURE A.6: Histogram of Turning Function Values for Initial Condition (4.2.1) with saturation function (4.2.3) when $q_a = 4, q_r = 1$

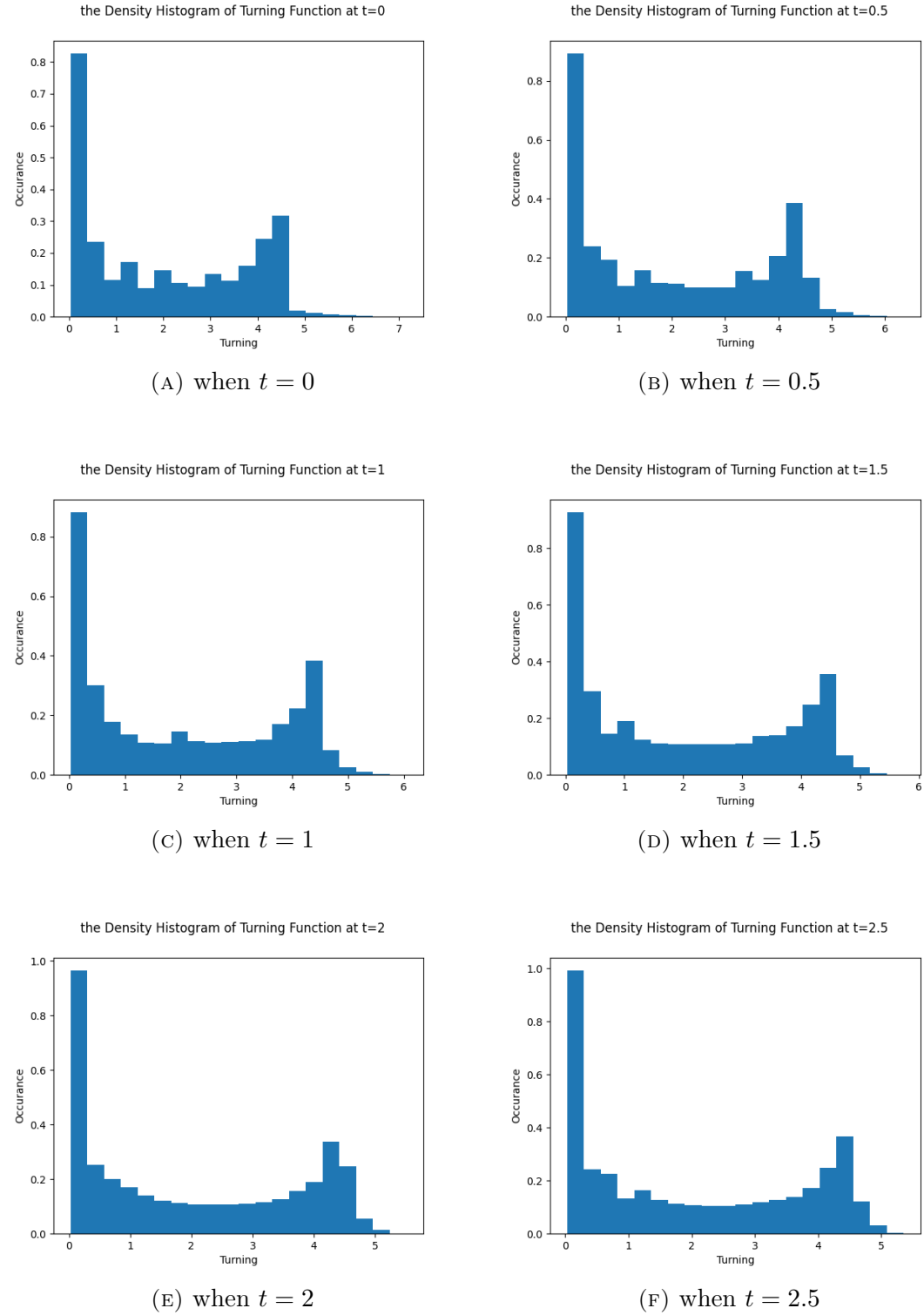


FIGURE A.7: Histogram of Turning Function Values for Initial Condition (4.2.1) with saturation function (4.2.4) when $q_a = 4, q_r = 1$

Appendix B

Truncation Error of Symmetry during Simulation

To calculate the asymmetry of the model, we set up a symmetric initial condition

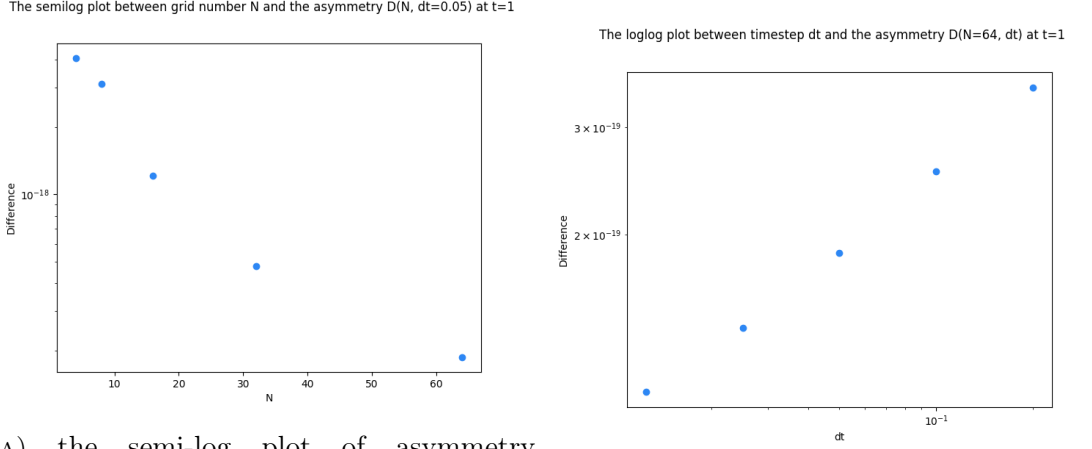
$$u(\phi, x_1, x_2) = \exp(-(x_1^2 + x_2^2)) \quad (\text{B.0.1})$$

which is a function with a Gaussian bump in the middle.

Then we calculate the asymmetry along the x-axis with different time step dt and different grid number N , which can be expressed as

$$D(N, dt) = \frac{\|u(\phi, x_1, x_2) - u(\pi - \phi, -x_1, x_2)\|}{\|u(\phi, x_1, x_2)\|} \quad (\text{B.0.2})$$

where the function $u(\phi, x_1, x_2)$ is calculated with different grid point number N and time step dt .



(A) the semi-log plot of asymmetry $D(N, dt = 0.05)$ vs. different grid number N at $t = 1$ (B) the log-log plot of asymmetry $D(N = 64, dt)$ vs. different time step dt at $t = 1$

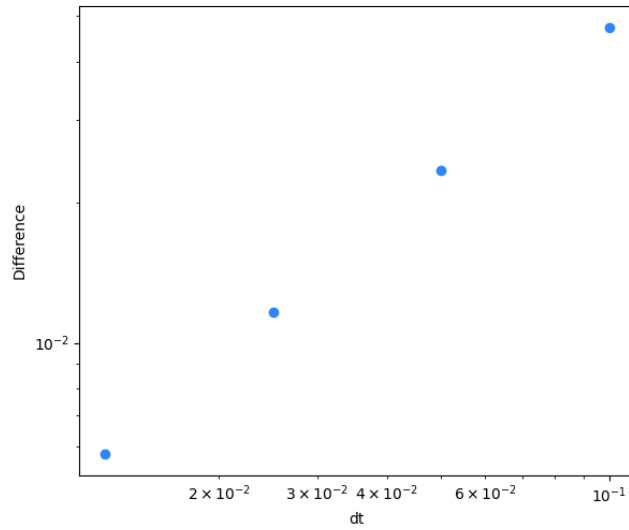
FIGURE B.1: The plot of asymmetry vs. dt and N of a model with symmetric initial condition (B.0.1). (A) shows the asymmetry $D(N, dt = 0.05)$ vs. N . (B) shows the asymmetry $D(N = 64, dt)$ vs. dt

From the plot B.1, the difference of the asymmetry at $t = 1$ are generally smaller than 10^{16} , which is preserved at machine precision.

The convergence test is also conducted for different dt values. The relative error is calculated as:

$$E(dt) = \|u_{dt}(\phi, x_1, x_2) - u_{dt}(\pi - \phi, -x_1, x_2)\| \quad (\text{B.0.3})$$

Then with a sequence of different time steps $dt = 0.2, 0.1, 0.05, 0.025, 0.0125$, the relative error $E(dt)$ is shown in Figure B.2.

The loglog plot between timestep dt and difference $|u_{dt1}-u_{dt2}|$ at $t=1$ FIGURE B.2: The magnitude of relative error at $t = 1$ with symmetric initial condition (B.0.1)

From Figure B.2, where the slope of the log-log plot approximately equals to 1 which is consistent with the Exponential Time Differencing method which is a first order simulation method.

Appendix C

Links of Supplementary Materials

C.1 Movies of the Results

The Movie for Initial Condition (4.1.1) with only transportation term:

https://youtu.be/ej2Segh4A_Y

The Movie for Initial Condition (4.1.1) with No saturation function:

<https://youtu.be/nmVe30sSfCI>

The Movie for Initial Condition (4.1.1) with saturation function (4.1.2):

<https://youtu.be/ovYIt1Ub0Fg>

The Movie for Initial Condition (4.2.1) with No saturation function when

$q_a = 2, q_r = 0.5$: <https://youtu.be/7bY-WNRRQu8>

The Movie for Initial Condition (4.2.1) with saturation function (4.1.2) when

$q_a = 2, q_r = 0.5$: <https://youtu.be/2m9vNRZEer8>

The Movie for Initial Condition (4.2.1) with saturation function (4.2.2) when

$q_a = 2, q_r = 0.5$: <https://youtu.be/lEkq3u27M2k>

The Movie for Initial Condition (4.2.1) with No saturation function when

$q_a = 4, q_r = 1$: <https://youtu.be/tkEJHhlTo1Y>

The Movie for Initial Condition (4.2.1) with saturation function (4.2.2) when

$q_a = 4, q_r = 1$: <https://youtu.be/ayngyuC6iaA>

The Movie for Initial Condition (4.2.1) with saturation function (4.2.3) when

$q_a = 4, q_r = 1$: <https://youtu.be/RDMMI6HezEM>

The Movie for Initial Condition (4.2.1) with saturation function (4.2.4) when

$q_a = 4, q_r = 1$: <https://youtu.be/tITYVBAE5Sk>

C.2 Codes for Simulations

Please see all the codes in this link:

https://github.com/A-Y-Qi/2022Thesis/tree/main/Thesis_Code